Isolation, Molecular Characterization, and Transplantation of PSA-NCAM^{-} Neural Crest Stem Cells from Human Pluripotent Stem Cells

Dongjin R. Lee

Department of Medical Science

The Graduate School, Yonsei University

Isolation, Molecular Characterization, and Transplantation of PSA-NCAM^{-} Neural Crest Stem Cells from Human Pluripotent Stem Cells

Directed by Professor Dong-Wook Kim

The Doctoral dissertation
submitted to the Department of Medical Science,
the Graduate School of Yonsei University
in partial fulfillment of the requirements for the degree of
Doctor of Philosophy

Dongjin R. Lee

December 2016

This certifies that
the Doctoral Dissertation of
Dongjin R. Lee is approved.

Thesis Supervisor:	Dong-Wook Kim
Thesis Committee Chair:	Joong Woo Leem
Thesis Committee Member #1:	Dong-Youn Hwang
Thesis Committee Member #2:	Han-Soo Kim
Thesis Committee Member #3:	Kyung-Hee Chun

The Graduate School
Yonsei University

December 2016

Acknowledgements

I would like to express my deepest gratitude to my advisor for his support throughout the research. I have always valued his counsel and guidance. I would also like to extend my appreciation to Professor Dong-Youn Hwang, Professor Han-Soo Kim, and Professor Dae-Sung Kim for their words of advice, guidance, and encouragement over the years which have made me a better scholar. I would like to express my sincere thanks to Dr. Jiho Jang for allowing me to grow as a person and experience fundamentals of professional practice.

My special thanks go to all my laboratory colleagues especially my teammates: Jeong-Eun Yoo, Sanghyun Park, and Hye-rim Shin. I am deeply indebted to my teammates as well as my fellow students: Jae Souk Lee, Junwon Lee, Sang-Hwi Choi, Eunhyun Ji, Hyesung Kang, Do-Hun Kim and Jiwon Lee who inspired me to keep moving forward and stay confident during the demanding and rigorous life of a Ph.D. student. To my friends back home, Jeremy Ng Wong Hing and Robert Novoa, I cannot thank you enough for your continuous generosity and friendship.

Last but not least, I must acknowledge and convey my heartfelt gratitude to God, my father, my mother, and my sister for their unconditional love and support. Finally, I would like to end with a quote; “work hard, be kind, and amazing things will happen.”

Table of contents

LIST OF FIGURES

LIST OF TABLES

Abstract

Isolation, Molecular Characterization, and Transplantation of PSA-NCAM$^-$ Neural Crest Stem Cells from Human Pluripotent Stem Cells

Dongjin R. Lee

Department of Medical Science
The Graduate School, Yonsei University

(Directed by Professor Dong-Wook Kim)

Tumorigenic potential of human pluripotent stem cells (hPSCs) is an important issue in clinical applications. To minimize and eliminate risk factors of tumor formation, strategies have been proposed to predifferentiate hPSCs into specific cell types *in vitro* or to isolate desired cell types via targeted cell sorting before their applications. Despite many efforts, PSC-derived neural precursor cell (NPC)-based therapeutic strategies have repeatedly resulted in tumor formation even though pluripotent cells were not detected when treating neurological disorders of the central nervous system (CNS) in animal models. In identifying risk factors for the tumorigenicity of NPC-based transplantation therapy, previous attempts have overlooked a key neurodevelopmental process - the emergence of multipotent neural crest stem cells (NCSCs) during the early neural induction process. Heterogeneity of the 'early' SOX1- and PAX6-expressing NPCs were carefully evaluated and found that polysialic acid-neural cell adhesion molecule (PSA-NCAM)-negative cells among the early NPCs caused

tumorigenesis, whereas PSA-NCAM^{+} cells were nontumorigenic. Comprehensive molecular profiling, global gene analysis, and multilineage differentiation of PSA-NCAM^{-} cells strongly support that they are multipotent NCSCs that could differentiate into both ectodermal and mesodermal lineages. The following study also demonstrated that the removal of PSA from PSA-NCAM^{+} cells leads to increased neural crest marker expression. Transplantation of PSA-NCAM^{-} cells in a gradient manner mixed with PSA-NCAM^{+} cells resulted in a proportional increase in mesodermal tumor formation and unwanted grafts such as PERIPHERIN^{+} cells or pigmented cells in the rat brain. Therefore, this study suggest that NCSCs are a new player for tumorigenesis in hPSC-derived NPC-based therapy and removal of PSA-NCAM^{-} cells eliminates the tumorigenic potential originating from NCSCs after transplantation into the CNS.

Key words: human pluripotent stem cells (hPSCs), neural precursor cells (NPCs), cell therapy, tumorigenesis, neural crest stem cells (NCSCs), polysialic acid-neural cell adhesion molecule (PSA-NCAM)

Isolation, Molecular Characterization, and Transplantation of PSA-NCAM$^-$ Neural Crest Stem Cells from Human Pluripotent Stem Cells

Dongjin R. Lee

Department of Medical Science
The Graduate School, Yonsei University

(Directed by Professor Dong-Wook Kim)

I. INTRODUCTION

In a process of attempting to mimic primary neuralization *in vivo*, studies have focused their attention on differentiating neural precursor cells (NPCs) from pluripotent stem cells (PSCs) for basic research and biomedical applications.[1] Given their advantages of a long-term expansion, high-culture purity, long-term neurogenic potentials, and their ability to survive cryopreservation, NPCs from human (h)PSC-derived neural rosettes, which represent neuroepithelial cells of unclosed and closed neural tubes, are an ideal cell source for biomedical applications.[2-4] Unfortunately, however, there have been reports of tumor formation after transplantation even in the absence of undifferentiated PSCs. Two distinctive types of tumors have been mainly described: neural overgrowth and mesodermal tumors. Neural rosettes (early NPCs) possess self-renewing multipotent characteristics, and a previous study showed neural overgrowth when they were transplanted *in vivo*.[3] Subsequent studies overcame this tumorigenic potential by further committing primitive NPCs to specific cell types and increasing differentiation efficiency.[5-7] Despite efforts to avoid pluripotent cell

contamination and NPC-neural overgrowth, researchers continue to report tumor formation post-transplantation of human embryonic stem cell (hESC)-derived NPCs or neuronal precursor cells in animal models of central nervous system (CNS) disorders containing chondrocytes, muscle fibers,[8] mesoderm-derived mature cartilage,[9] and pigmented cells.[10]

Meanwhile, *in vitro* studies of neural induction from hPSCs have suggested that radial arrangements of columnar neuroepithelial cells, termed neural rosettes can differentiate towards peripheral nervous system (PNS) lineages[2, 11] and reported evidence of neural crest-like cells within the neural rosette cultures.[3, 12, 13] During embryonic development, transient and highly migratory neural crest stem cells (NCSCs) give rise to melanocytes, neurons and glial cells of PNS, as well as connective tissue cells, chondrocytes, osteocytes, and adipocytes of the craniofacial complex.[14] Neural crest cells share the same developmental origin of gastrula ectoderm as the neuroectoderm and hold multipotency yielding cells of mesodermal and ectodermal lineages that comprise the PNS;[15] therefore, it is hypothesized that neural rosette cultures could be heterogeneous and may contain NCSCs that may cause mesodermal tumor growth and introduce unwanted cell populations (e.g., pigmented cells) after transplantation into the CNS.

In examining the heterogeneity of neural rosettes, a subset (~21%) of PSA-NCAM-negative (PSA-NCAM$^-$) cells was identified. Interestingly, these cells did not express an early marker of neuroectoderm, (Pax6), but they possessed NCSC characteristics. When isolated from neural rosette populations, PSA-NCAM$^-$ cells showed pronounced multipotent phenotypes when directed to differentiate. Because PSA-NCAM$^-$ cells carry multipotency of NCSCs, it was postulated that PSA-NCAM$^-$ cells were responsible for the formation of mesodermal tumors and unwanted grafts after hPSC-derived NPC transplantation. To test the hypothesis, PSA-

NCAM$^-$ cells mixed with PSA-NCAM$^+$ cells were transplanted in a gradient manner in the rat brain. The investigation revealed a proportional increase in mesodermal tumor formation, the appearance of pigmented cells and PERIPHERIN$^+$ grafts in the brain. These results indicate that NCSCs classified as PSA-NCAM$^-$ cells can be a new target for tumor prevention in hPSC-derived-NPC-based therapy and that removal of PSA-NCAM$^-$ cells would prevent the introduction of mesodermal tumor and unwanted graft formations after NPC transplantation in the CNS.

II. MATERIALS AND METHODS

1. Stem cell culture and differentiation

Undifferentiated hESCs (H9 [WA09; WiCell Inc.], Madison, Wisconsin, USA) were cultured on mouse STO fibroblasts (ATCC, Manassas, Virginia, USA) under previously described growth conditions.[16] To induce neural rosettes, EBs were cultured in suspension for 4 days in hESC media excluding basic Fibroblast Growth Factor (bFGF) but supplemented with 5 μM dorsomorphin (DM) (Calbiochem, San Diego, California, USA) and 5–10 μM SB431542 (SB) (Sigma-Aldrich, St. Louis, Missouri, USA). On the fourth day, EBs were attached in Matrigel-coated culture dishes (BD Biosciences, San Jose, California, USA) in DMEM/F12 N2 supplemented media (N2 media) with 20 ng/mL bFGF (R&D Systems, Minneapolis, Minnesota, USA) and 19–21 μg/mL human insulin solution (Sigma-Aldrich) for another 5 days. The emerged rosette structures were mechanically isolated using pulled glass pipettes within the EB colonies, and isolated neural rosette clumps were replated in Matrigel-coated dishes. Replated neural rosettes were then expanded for an additional 6–7 days at 90% confluence. PSA-NCAM$^+$ and PSA-NCAM$^-$ cells were isolated via Magnetic Activated Cell Sorting (MACS) (Miltenyi Biotec, Cologne, Germany) as previously described.[12] Isolated cells were plated in Matrigel-coated dishes at a density of 1–1.55 × 10^5 and 1–1.25 × 10^5 cells/cm^2 for PSA-NCAM$^+$ and PSA-NCAM$^-$ cells, respectively. Although PSA-NCAM$^-$ cells were maintained in N2 media with insulin, 20 ng/mL bFGF, and 10 ng/mL epidermal growth factor (EGF) (Peprotech, Rocky Hill, New Jersey, USA), the positive cells were maintained in DMEM/F12 N2 and B27 without vitamin A supplemented media (N2B27 media) with 20 ng/mL bFGF. Media

were replaced daily. To isolate NCSCs from the propagated neural rosette population, additional two-step MACS (CD271; CD57 MicroBeads, Miltenyi Biotec) was performed following the same procedures with a slight modification. Isolated $CD271^+$ cells were washed with calcium-, magnesium-free, and phenol red-free HBSS (Gibco-Thermo Fisher Scientific, Waltham, Massachusetts) twice. The positive cells then eluted with 1× TrypLE Express (Gibco-Thermo Fisher Scientific) and nutated in TrypLE Express for 3-5 min.[17] To stop the reaction, the cells were washed with 2% bovine serum albumin (BSA)-phosphate-buffered saline (PBS) solution followed by 1× cold PBS wash before attaching CD57 MicroBeads and application over a second column. For peripheral neuron differentiation, PSA-$NCAM^-$ cells (passages 6-8) were seeded in fibronectin- or poly-L-ornithine/laminin-coated four-well dishes in N2B27 media with brain-derived neurotrophic factor (10 ng/mL), glial cell line-derived neurotrophic factor (10 ng/mL), nerve growth factor (10 ng/mL), neurotrophin-3 (10 ng/mL) (all Peprotech), ascorbic acid (200 μM; Sigma-Aldrich), and DAPT (2.5 μM; Calbiochem).[18] Differentiation was induced for 20 days before immunocytochemistry assays were performed. For mesenchymal differentiation, PSA-$NCAM^-$ cells were cultured in N2 media for 24 hr and switched to DMEM GlutaMAX supplemented with 10% FBS and 5 μg/mL gentamicin. Adipocyte, chondrocyte, and osteocyte differentiations were carried out according to the manufacturer's instructions using StemPro® Differentiation Kits (Invitrogen-Thermo Fisher Scientific). To remove PSA from the surfaces, EndoN (Abc Scientific, Glendale, California, USA), which specifically degrades linear α-2,8-linked PSA, was introduced to PSA-$NCAM^{+/-}$ cells for 24 (data not shown) or 48 hr.

2. Immunocytochemistry and flow cytometry

Cells were fixed in 4% paraformaldehyde- PBS solution. For visualization of intracellular markers, cells were permeabilized with 0.1% Triton X-100-PBS solution, blocked with 2% BSA-PBS solution for 1 hr at room temperature and incubated overnight at 4°C with primary antibodies: AFP (Santa Cruz, Dallas, Texas, USA); OCT4 (Santa Cruz); AP2 (DSHB, Iowa City, Iowa, USA); p75 (Advance Targeting Systems, San Diego, California, USA) BRACHYURY (R&D Systems); p75-AF647 (BD Biosciences); CALPONIN (Sigma-Aldrich); p75-Microbead (Miltenyi Biotec); CD105-FITC (Accurate Chemical, Westbury, New York, USA); PAX6 (DSHB); CD29-PE (Accurate Chemical); PERIPHERIN (Merck Millipore, Darmstadt, Germany); CD44-PE (Accurate Chemical, Westbury, New York, USA); PLZF (Merck Millipore); CD73-PE (BD Biosciences); PSA-NCAM (Merck Millipore); CD90-FITC (Immunotech); PSA-NCAM Microbead (Miltenyi Biotec); FOXA2 (Santa Cruz); RUNX2 (R&D Systems); HNA (Merck Millipore); SMAα (Sigma-Aldrich); HNK1 (Sigma-Aldrich); SOX1 (Merck Millipore); HNK1-FITC (BD Biosciences); SOX17 (R&D Systems); HNK1-Microbead (Miltenyi Biotec); SOX2 (Merck Millipore); Ki67 (Vision Biosystems); SSEA4 (Merck Millipore); NANOG (Abcam); Tra-1-81 (Merck Millipore); NCAM (Merck Millipore); TuJ1 (Covance); NESTIN (Merck Millipore); ZO-1 (BD Biosciences & Invitrogen-Thermo Fisher Scientific). Appropriate fluorescence-tagged secondary antibodies (Molecular Probes-Thermo Fisher Scientific and Vector Laboratories, Burlingame, California, USA) were used for visualization. Cells were mounted in 4',6-diamidino-2-phenylindole mounting medium (Vector Laboratories), and images were obtained using an Olympus IX71 microscope equipped with a DP71 digital camera or Olympus FSX100

system. MetaMorph Microscopy Automation & Image Analysis Software (Molecular Devices, Sunnyvale, California, USA) were used to count positive cells in 7-10 randomly selected images at a final magnification of ×200 from each of three independent experiments. For flow cytometry, cells were dissociated into single cells using Gibco® Cell Dissociation Buffer (Invitrogen-Thermo Fisher Scientific) and incubated in 1% BSA-PBS solution with the appropriate antibodies. For unconjugated primary antibodies, the cells were incubated with Alexa-Flour 488-conjugated anti-mouse IgG/IgM (Molecular Probes) for raising suitable secondary antibodies. Flow cytometry was performed using FACSCalibur (BD Biosciences) and analyzed using WinMDI 2.8 or with FACSVerse (BD Biosciences) and analyzed using FlowJo software.

3. Gene expression analyses and transcription profiling

Total RNA was isolated using the Easy-Spin® Total RNA Extraction Kit (iNtRON). cDNA was synthesized from 1 μg of total RNA using the PrimeScript™ RT Master Mix (Takara Bio Inc., Kusatsu, Shiga, Japan). mRNA levels were quantified by real-time RT-PCR assays using the SYBR Premix Ex Taq™ (Takara Bio Inc.) and CFX96 Real-Time System (Bio-Rad, Hercules, California, USA). Ct values for each targeted gene were normalized according to those of β-actin, and the normalized expression levels of the targeted genes were compared between the sorted/unsorted samples and control samples based on the comparative Ct method. Data are expressed as the mean relative expression ± standard error of the mean (SEM) from three independent experiments. Semiquantitative PCR was performed using the EmeraldAMP GT PCR master mix (Takara Bio Inc.) in the GeneAmp PCR System 2720 (Applied Biosystems-Thermo Fisher

Scientific). The sequences of the primers used to characterize H9, neural rosettes, and PSA-NCAM$^{+/-}$ cells are listed in Table 5, 6.

For microarray analysis, 10 μg of total RNA from each sample was processed and analyzed by Macrogen Inc. (Seoul, Korea), and the samples were hybridized to the Human HT-12 Expression v.4.0 bead array. For clustering analysis, the normalized data were narrowed down to 20,287 using a cutoff based on fail.count < 6. We found 1,178 out of 20,287 genes with $P > 0.05$ (local-pooled error test adjusted P-value cutoff < 0.05). GO analyses were performed using DAVID (Database for Annotation, Visualization and Integrated Discovery). Significantly upregulated genes were compared against DAVID's GO FAT database to clarify biological meanings. The P values were derived using Fisher's exact tests ($P < 0.01$ and fold-enrichment ≥2.0), and the corrected P values were applied to multiple testing corrections using the Benjamini-Yekutieli method.

4. *in vivo* transplantation and immunohistochemistry

Adult male Sprague-Dawley rats weighing 200–250 g were used at the time of transplantation (Orient Bio Inc., Seongnam, Korea). Propagated neural rosettes (d7) and PSA-NCAM$^{+/-}$ cells were dissociated into single cells using Accutase (Merck Millipore), and then suspended in Dulbecco's PBS to a final cell concentration of 1×10^5 cells/μl. Three microliters of the cell suspension was stereotaxically transplanted per rat at the following coordinates: AP +0.05, ML +0.30, DV -0.40 and -0.50. Next, 30 mg/kg Zoletil® (Virbac, Carros, France) was combined with 10 mg/kg Rompun® (Bayer, Leverkusen, Germany) for anesthesia, and 10 mg/kg cyclosporine A (Chong Kun Dang, Seoul, Korea) was intraperitoneally administered 24 hr pre-transplantation and every day thereafter until the rats were sacrificed.

Ten wk post-transplantation, the rats were anesthetized with the anesthetic mixture (Zoletil:Rompun) and transcardially perfused with 0.9% saline solution followed by 4% paraformaldehyde. Removed brains were post-fixed overnight and cryoprotected in 30% sucrose-PBS solution. Cryoprotected brains were embedded in FSC 22® compound (Leica, Nußloch, Germamy), and serial coronal sections were sliced at 16–20 μm using a cryostat (Thermo Fisher Scientific). Progressive H&E staining was performed, and immunohistochemistry was carried out as previously described.[12] Lineages of structures found in each graft were determined based on H&E sections first, followed by immunofluorescence staining targeting specific antigens with appropriate antibodies that were mentioned previously.

5. Statistical analysis

Data are shown as the mean ± SEM of at least three independent experiments. Data were analyzed using the paired/unpaired, two-tailed Student's *t*-tests or analyses of variance (ANOVA) when two or more groups were involved.

III. RESULTS

1. PSA-NCAM-targeted Cell Sorting Isolates Neural Crest-like Cells from Heterogeneous Neural Rosette Populations

Neural induction and neural rosette isolation from hPSCs were performed as described in the previous reports (Figure 1A).[11, 12] The expanded neural rosette cultures expressed neuroectodermal and neuroepithelial markers, including sex determining region Y-box-2 (SOX2), NESTIN, SOX1, and paired box 6 protein (PAX6) (Figure 1B-D). Tight junction protein (ZO-1) and promyelocytic leukemia zinc finger (PLZF) expression confirmed the neural rosette characteristics (Figure 1D, E), and the previously defined "rosette-specific markers" were also maintained throughout expansion (Figure 2A).[3] As previously described, the neural rosette cultures appeared to be mainly PSA-NCAM$^+$ and consisted of PAX6$^+$ neuroepithelial cells (Figure 1F).[12] Despite the predominant PSA-NCAM$^+$ expression within the cultures, negative cells were observed around the outer boundary of PSA-NCAM$^+$ rosette core and these cells expressed the neural crest marker p75 (Figure 1G). Expression of AP2 (a neural crest lineage marker) was also observed in SOX1$^-$ cells scattered around SOX1$^+$/AP2$^-$ neural rosettes (Figure 1H). AP2$^+$ cells remained when the neural rosette cultures were dissociated into single cells to examine the characteristics of individual cells (Figure 1I). These results indicated that the neural rosette cells were heterogeneous in terms of having neural crest-like characteristics and could be divided into PSA-NCAM$^+$ and PSA-NCAM$^-$ populations.

The heterogeneous neural rosette cultures were divided into two different populations via magnetic activated cell sorting (MACS) using PSA-NCAM antibodies. The potential presence of residual undifferentiated cells

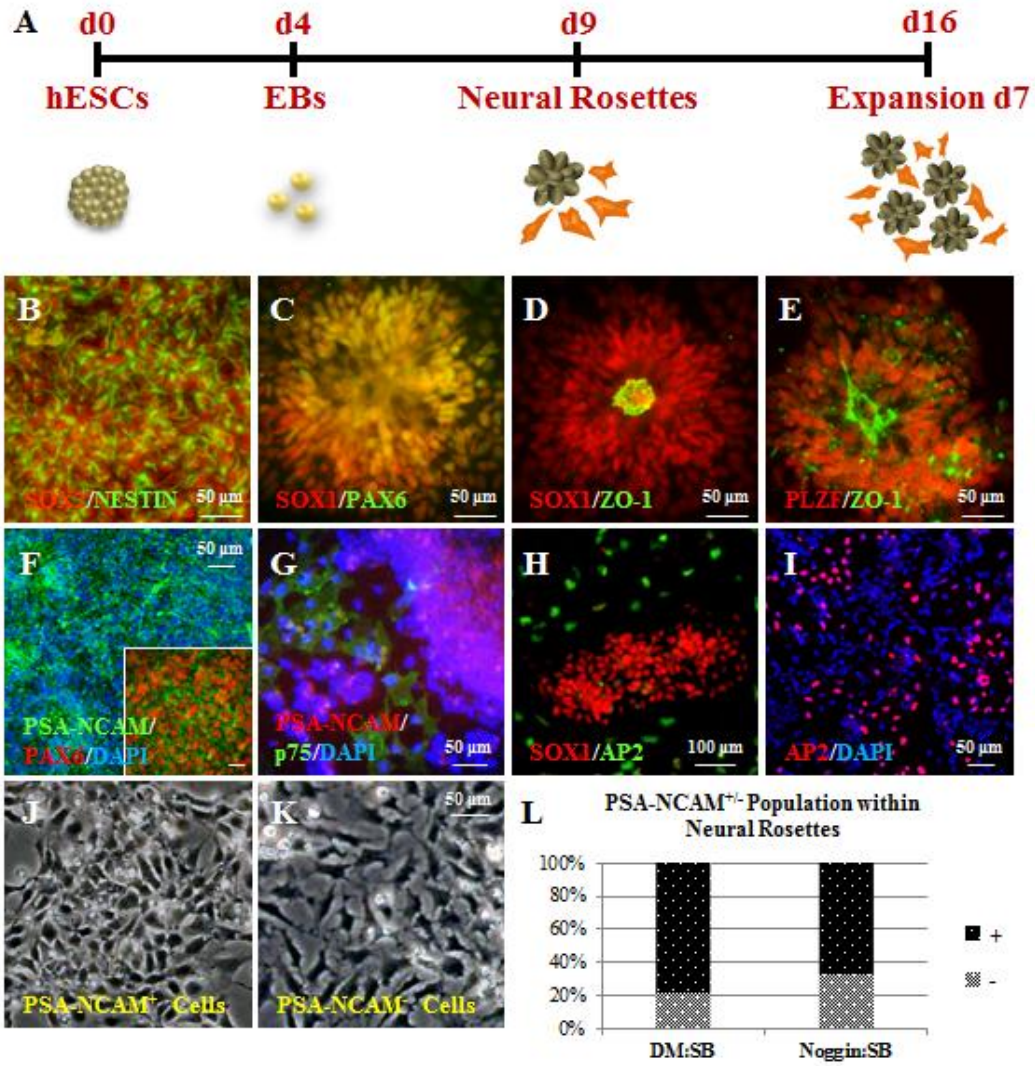

Figure 1: PSA-NCAM-targeted cell sorting can isolate neural crest-like cells from heterogeneous neural rosette cultures. (A) Timeline of neural rosette generation method. (B and C) $SOX2^+/NESTIN^+$ and $SOX1^+/PAX6^+$ neuroepithelial cells were observed in the expanded neural rosette cultures. (D and E) Coexpression of SOX1/ZO-1 and PLZF/ZO-1 identified the physical property of neural rosettes. (F) Predominant $PSA\text{-}NCAM^+$ expression within the neural rosette population that was comprised of $PAX6^+$ neuroepithelial cells. (G) $p75^+$ cells were observed peripheral to the $PSA\text{-}NCAM^+$ neural rosette core. (H) $AP2^+/SOX1^-$ cells were observed peripheral to the $SOX1^+$ neural rosette core. (I) $AP2^+$ cells were identified at a single-cell level. (J and K) $PSA\text{-}NCAM^+$ cells showed neural rosette morphologies, whereas negative cells exhibited neural crest-like physical characteristics. (L) Among the neural rosette cultures, the populations that were positive and negative for PSA-NCAM comprised 79% and 21%, respectively. Another common method for neural induction using Noggin and SB431542 yielded ~30% $PSA\text{-}NCAM^-$ cells. The error bars indicate the SD (n = 4).

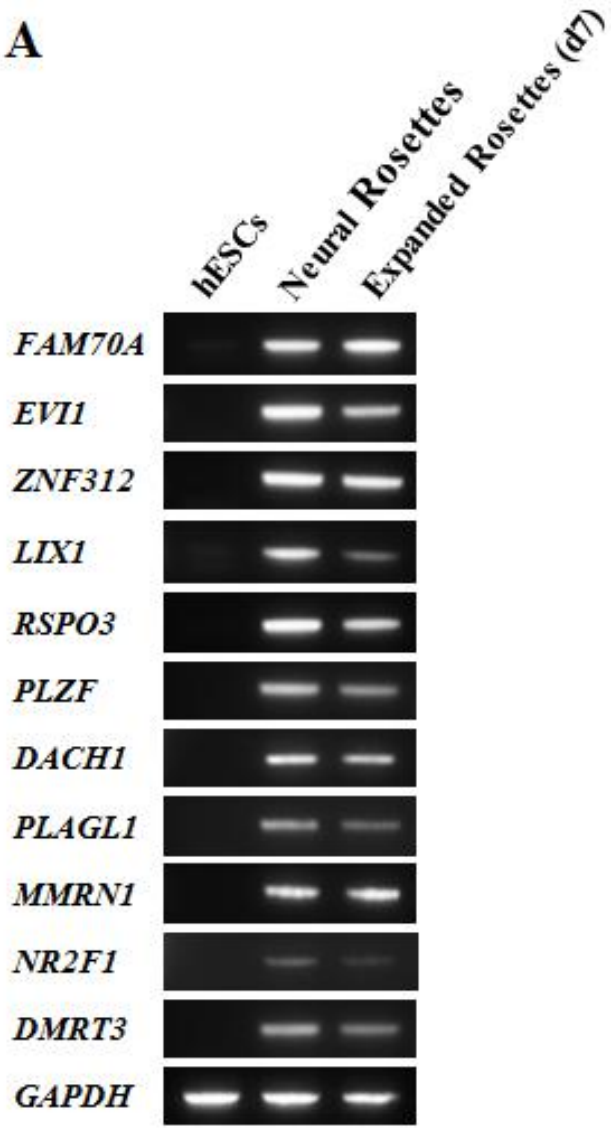

Figure 2: hESC-derived neural rosettes express the rosette-specific genes. (A) Semiquantitative RT-PCR analysis was performed to observe expression of genes previously described as "rosette-specific". While no expression was detected in hESCs (H9), hESC-derived neural rosettes expressed the rosette-specific genes and the expression was maintained throughout the 7-day expansion.

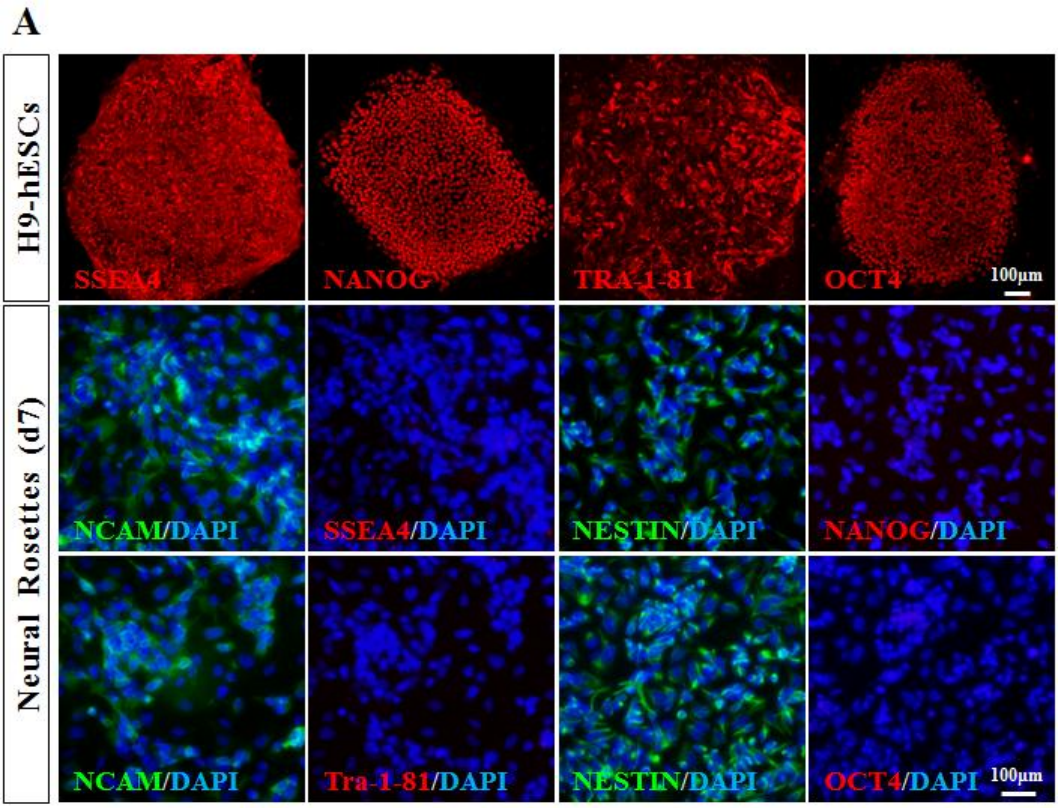

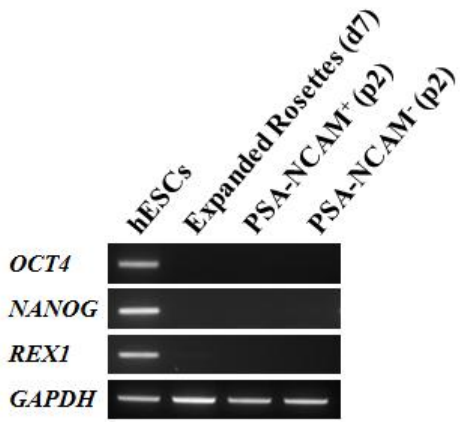

Figure 3: Expanded neural rosettes before sorting show no signs of pluripotency. (A) As shown via immunocytochemistry, pluripotency markers including SSEA4, NANOG, TRA-1-81, and OCT4 were targeted in hESCs (H9) and neural rosettes. hESCs expressed all four pluripotency markers; however, neural rosettes showed no expression of pluripotency markers while showing positive expression for NCAM and NESTIN. (B) Semiquantitative RT-PCR analysis also indicated no expression of pluripotency marker genes *OCT4*, *NANOG*, and *REX1* in neural rosettes, PSA-NCAM^{+} cells, and PSA-NCAM^{-} cells unlike hESCs. *GAPDH* is shown at the bottom as a loading control for each lane.

was examined prior to MACS; however, no PSCs were detected in the neural rosette population or the sorted cells (Figure 3A, B). PSA-NCAM$^+$ cells had the physical appearance of polarized neural rosette cells and made of 79% of the total neural rosette population, whereas PSA-NCAM$^-$ cells had the morphology of neural crest-like cells and account for the remaining 21% of the total population (n = 4, Figure 1J-L). The percentage of culture population suggests that expanded neural rosette cultures contain approximately 21% PSA-NCAM$^-$ cells with a non-neural rosette appearance.

2. Molecular Characterization and Global Gene Expression Analysis of PSA-NCAM$^-$ Show NCSC Characteristics

The composition of PSA-NCAM$^-$ cells were analyzed more closely because they exhibit a neural crest-like cell morphology that is not observed in neural cells of the CNS. First, the percentage of cells from the neural crest lineage was examined using three neural crest markers: p75, HNK1, and AP2. Flow cytometry showed that up to 95.8% (n = 4) of the PSA-NCAM$^-$ population was p75$^+$, whereas 96.8% of this population was HNK1$^+$ (Figure 4A, B). PSA-NCAM$^-$ cells derived from the human induced pluripotent stem cell (iPSC) line WT-iPSCEpi3 provided similar results (Figure 5A-D). According to the fluorescence-activated cell sorting (FACS) results, the pluripotent cell marker, SSEA4 was not expressed in PSA-NCAM$^-$ cells (Figure 4C). Additionally, 86.9% of the initial passage (p0) of PSA-NCAM$^-$ cells were positive for AP2, and this increased to 92.3% as the cells were further subcultured (p2), suggesting progressive specification towards neural crest cells (n = 3, $P < 0.05$). The quantification of cells expressing Ki67, a cell cycle marker for an all-active phase, showed that 88.9% of AP2$^+$/PSA-NCAM$^-$ cells were in a proliferative state (Figure 4D). Immunocytochemical

analysis of the PSA-NCAM$^-$ cells verified their neural crest identities (Figure 4E-H). To further characterize the PSA-NCAM$^-$ cells, real-time reverse transcription polymerase chain reaction (RT-PCR) analysis was performed targeting key transcripts related to neural crest identity. PSA-NCAM$^-$ cells showed elevated levels of *p75* and *AP2* compared with neural rosette cells and PSA-NCAM$^+$ cells (Figure 6A, B). The expression level of *cMYC,* an important factor for pluripotency and the earliest expressed neural crest specifier[19], was consistent throughout the targeted cells, with the exception of PSA-NCAM$^+$ cells (Figure 6C). PSA-NCAM$^-$ cells displayed elevated levels of transcripts responsible for pre-migratory and migratory NCSCs (Figure S3D-H), and the levels of epithelial-mesenchymal transition (EMT) regulatory factors such as *TWIST1*, *SLUG*, and *SNAIL* increased with the passage number (p2 vs. p4) (Figure 6D-F).[19] These results provide molecular evidence that multiple neural crest marker genes are predominantly expressed in PSA-NCAM$^-$ cells compared to PSA-NCAM$^+$ cells.

When isolating NCSCs from hPSCs *in vitro*, p75$^+$ or p75$^+$/HNK1$^+$ cells were targeted from differentiated cultures as described in previous reports.[13, 20-23] Because this study is providing the first evidence that PSA-NCAM$^-$ cells are NCSCs, PSA-NCAM$^-$ cells were compared to the previously established NCSCs, p75$^+$/HNK1$^+$ cells. Two-step MACS sorting was performed to obtain p75$^+$/HNK1$^+$ cells and their purity was confirmed with flow cytometry and immunocytochemistry (Figure 4I-L). Transcriptome analyses were performed in triplicate to compare the global gene expression patterns of neural rosettes, PSA-NCAM$^+$, PSA-NCAM$^-$, and p75$^+$/HNK1$^+$ cells (Figure 4M-R). Hierarchical clustering analysis of 20,287 (fail.count < 6) normalized genes was performed using complete linkage and Euclidean distance as measures of similarity. The expressed transcripts were clustered into two expression groups of neural rosettes and PSA-NCAM$^+$ cells versus

PSA-NCAM$^-$ cells and p75$^+$/HNK1$^+$ cells (Figure 4M).

Next, genes upregulated in PSA-NCAM$^+$, PSA-NCAM$^-$, and p75$^+$/HNK1$^+$ cells were identified relative to neural rosettes (fold change > 2.0). As shown in the Venn diagrams in Figure 4N, 1 gene in the PSA-NCAM$^+$ group, 104 genes in the PSA-NCAM$^-$ group, 67 genes in the p75$^+$/HNK1$^+$ group, and 143 genes in both the PSA-NCAM$^-$ group and the p75$^+$/HNK1$^+$ group were expressed at higher levels than in the neural rosette group. Furthermore, genes that were upregulated in PSA-NCAM$^-$ and p75$^+$/HNK1$^+$ cells relative to PSA-NCAM$^+$ cells were identified (fold change > 2.0). 113 genes in the PSA-NCAM$^-$ group, 56 genes in the p75$^+$/HNK1$^+$ group, and 144 genes in both the PSA-NCAM$^-$ and p75$^+$/HNK1$^+$ groups were upregulated compared to the PSA-NCAM$^+$ group (Figure 4O). Gene Ontology (GO) analysis of the 257 genes activated in PSA-NCAM$^-$ cells and 200 genes activated in p75$^+$/HNK1$^+$ cells identified a number of skeletal system-associated, neural tube-associated, mesenchyme-associated, and neural crest cell-associated terms (Table 1, 2). GO analysis also indicated that PSA-NCAM$^-$ and p75$^+$/HNK1$^+$ cells were more likely to undergo EMT in comparison to PSA-NCAM$^+$ cells (Table 3, 4). The scatter plots also showed that PSA-NCAM$^-$ and p75$^+$/HNK1$^+$ cells were the most similar of all the groups (Figure 4P-R). In summary, the global gene expression profiles of PSA-NCAM$^-$ and p75$^+$/HNK1$^+$ cells revealed analogous molecular characteristics between the two groups in a comparison to PSA-NCAM$^+$, further confirming the authenticity of the NCSC characteristics of PSA-NCAN$^-$ cells.

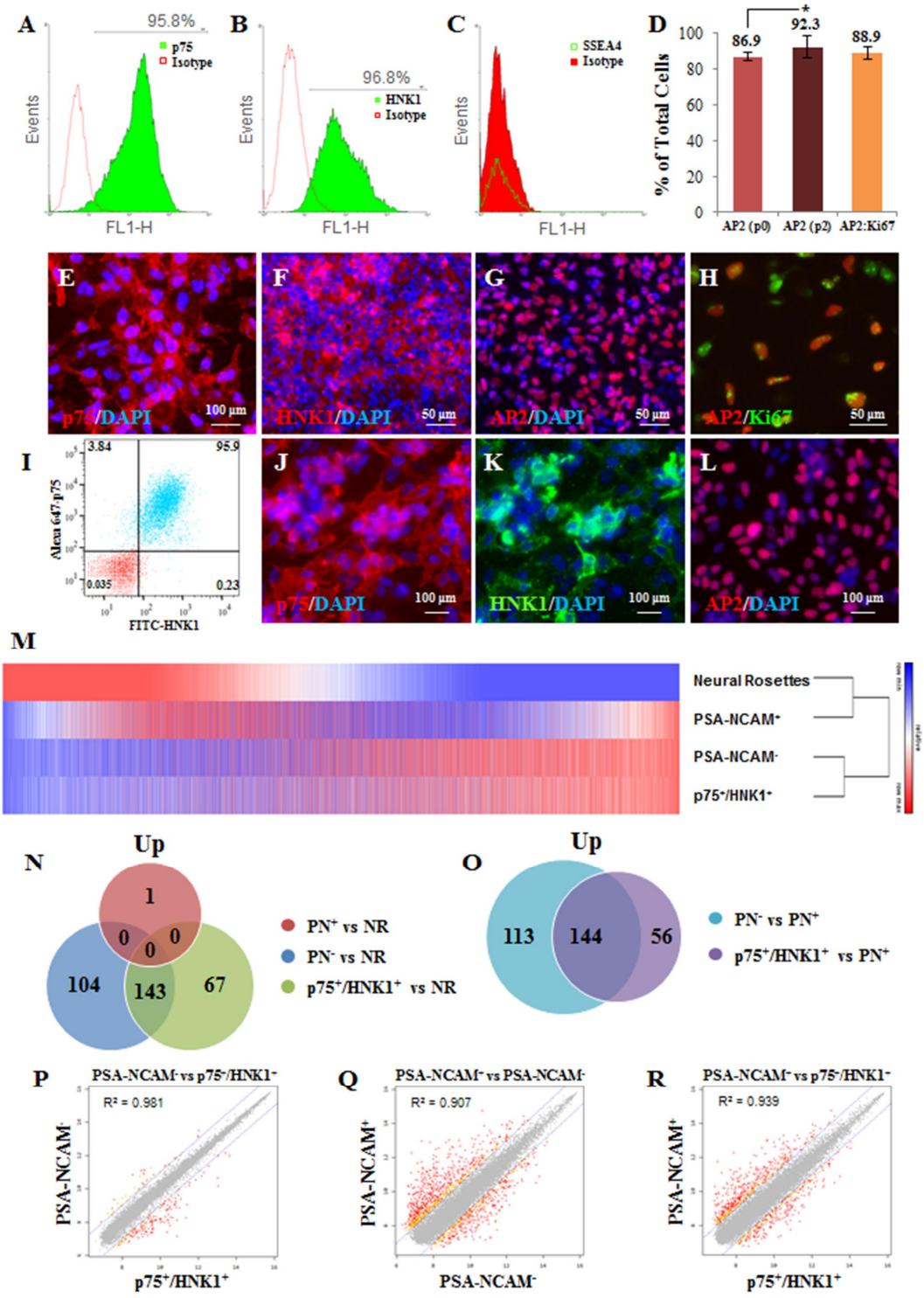

Figure 4: Molecular characterization of PSA-NCAM$^-$ cells and global gene expression pattern analysis for PSA-NCAM$^{+/-}$ and p75$^+$/HNK1$^+$ cells. (A and B) Flow cytometry analysis targeting p75 and HNK1 in PSA-NCAM$^-$ cells. (C) No SSEA4$^+$ cells were observed in PSA-NCAM$^-$ cells. (D) Within the PSA-NCAM$^-$ culture, 86.9% of unpassaged cells (p0) were AP2$^+$, and the positivity increased to 92.3% as the cells were passaged (p2). 88.9% of AP2$^+$ PSA-NCAM$^-$ cells were Ki67$^+$ (*, $P < 0.05$, unpaired Student's *t*-test, Mean ± SD, n = 3). (E-H) Immunocytochemistry analysis of PSA-NCAM$^-$ cells showed strong expression of p75, HNK1, and AP2 with Ki67 activity.
(I-L) Validation of two-step MACS isolated p75$^+$/HNK1$^+$ cells via flow cytometry (95.9%) and immunocytochemistry analysis. (M) Hierarchical clustering of the 20,287 genes was performed using the mean signal intensities of three biological replicates for each group (fail.count < 6). (N) Venn diagram of genes upregulated in PSA-NCAM$^+$, PSA-NCAM$^-$, and p75$^+$/HNK1$^+$ groups relative to the neural rosette group (PN$^+$: PSA-NCAM$^+$, PN$^-$: PSA-NCAM$^-$, and NR: neural rosettes). P-value indicates the significance of overlap determined from hypergeometric distribution analysis (blue and green overlap, $P < 8.64E^{-64}$). (O) Genes with increased expression in the PSA-NCAM$^-$ and p75$^+$/HNK1$^+$ groups in a comparison to PSA-NCAM$^+$ group were compared using a Venn diagram ($P < 2.13E^{-66}$). (P-R) Scatter plots were drawn identifying r^2 values for each comparison.

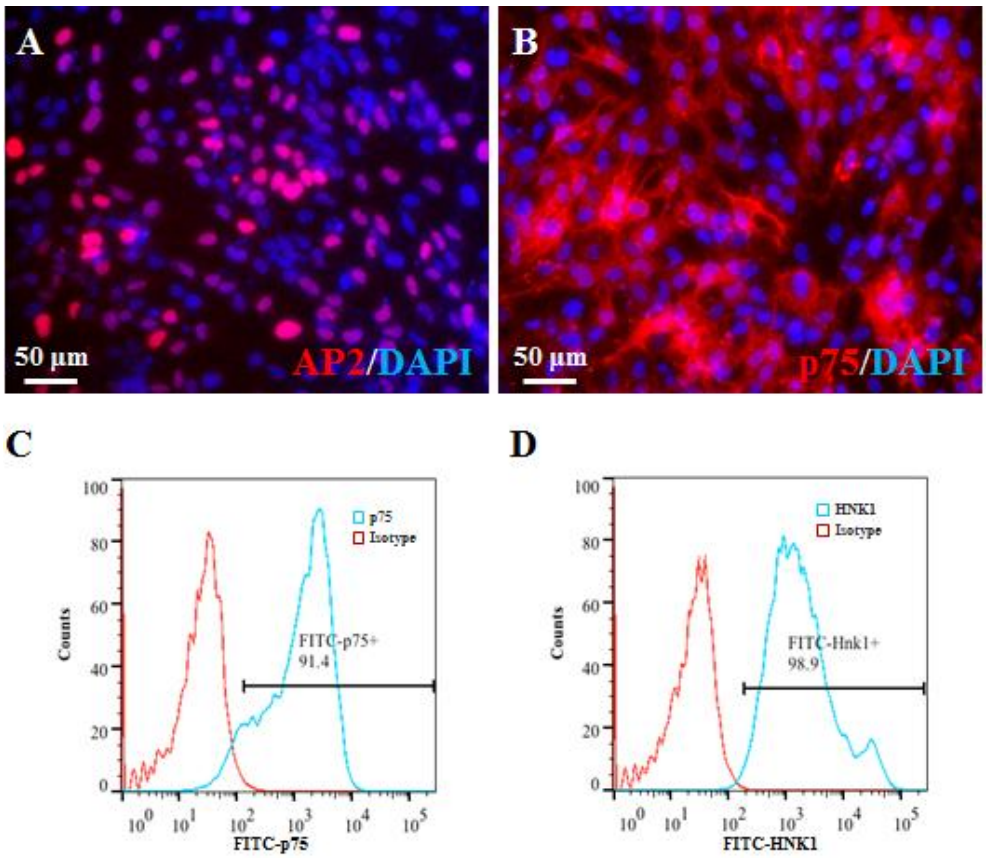

Figure 5: WT-iPSCEpi3-derived PSA-NCAM$^-$ cells express neural crest markers and the population of NCSCs is compatible to that of hESC-derived PSA-NCAM$^-$ cells. (A, B) Immunocytochemistry analysis of iPSC-derived PSA-NCAM$^-$ cells for markers of NCSC; AP2 and p75. (C, D) Flow cytometry analysis for p75 and HNK1 of PSA-NCAM$^-$ cells (p1). Plots shown are representative of results from three different WT-iPSCEpi3-derived PSA-NCAM$^-$ cultures.

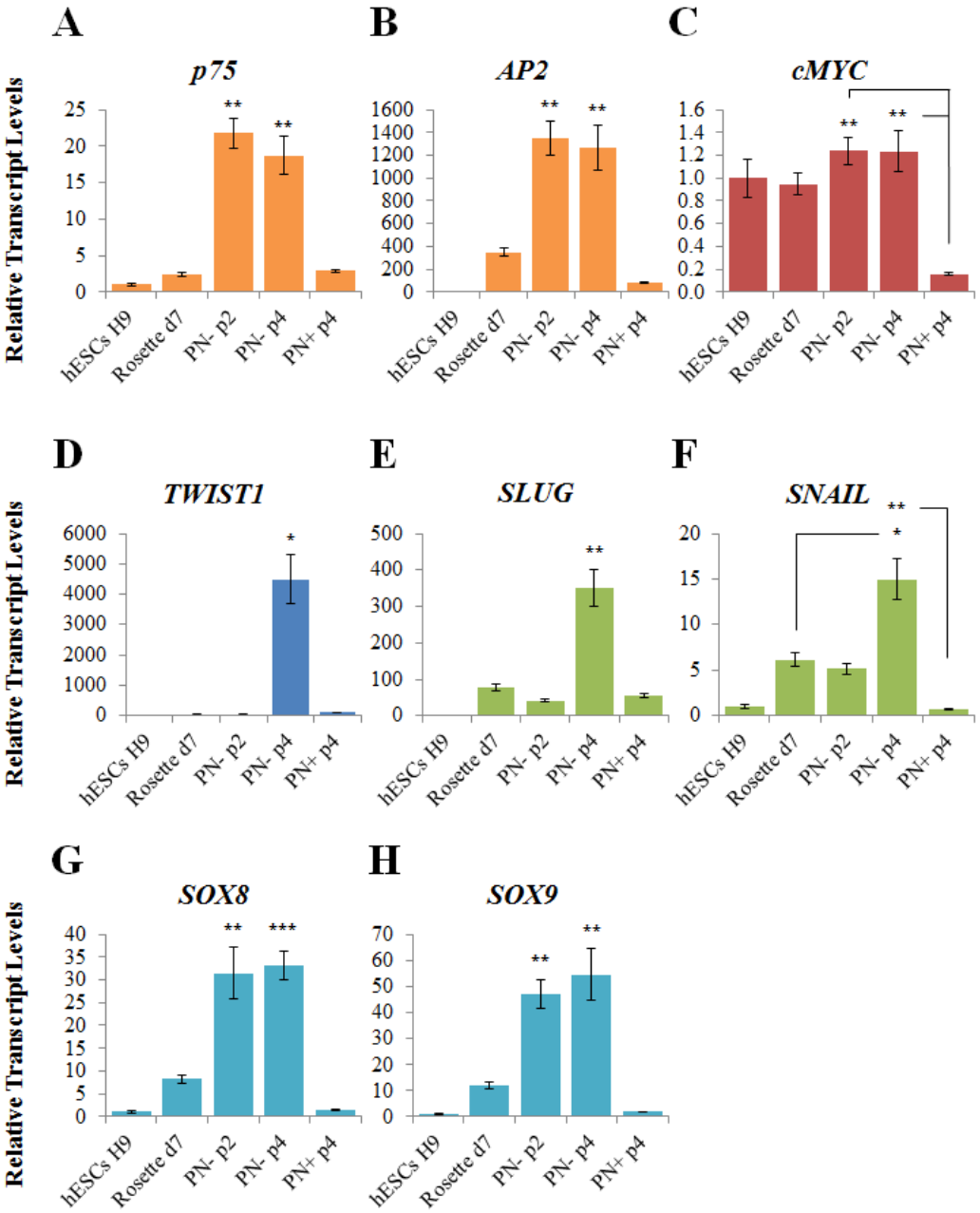

Figure 6: Real-time RT-PCR analysis of key transcripts that are related to neural crest identity in PSA-NCAM$^-$ cells versus PSA-NCAM$^+$ cells. (A, B) RT-PCR assay for *p75* and *AP2* indicated increased expression in PSA-NCAM$^-$ cells (p2 and p4) relative to parent neural rosettes and PSA-NCAM$^+$ cells (Mean ± SEM, n = 3 independent experiments). (C) PSA-NCAM$^+$ cells showed a decreased expression level of *cMYC* compared to all targeted cells (Mean ± SEM, n = 3 independent experiments). (D-F) EMT regulatory factors including *TWIST1*, *SLUG*, and *SNAIL* were highly expressed in passaged (p4) PSA-NCAM$^-$ cells (Mean ± SEM, n = 3 independent experiments). (G, H) Neural crest precursor specifiers such as *SOX8* and *SOX9* also showed higher expression level in PSA-NCAM$^-$ cells relative to neural rosettes and PSA-NCAM$^+$ cells (*, $P < 0.05$; **, $P < 0.01$; ***, $P < 0.001$, Student's *t*-test, Mean ± SEM, n = 3 independent experiments).

Table 1. Gene Ontology Analysis of 257 Genes upregulated in PSA-NCAM$^-$ cells relative to PSA-NCAM$^+$ cells

GO Accession	Gene Ontology (GO) Term	Corrected P Value
GO:0008284	positive regulation of cell proliferation	1.84E-08
GO:0042127	regulation of cell proliferation	3.88E-08
GO:0001501	skeletal system development	2.30E-07
GO:0048705	skeletal system morphogenesis	7.02E-06
GO:0048754	branching morphogenesis of a tube	1.11E-05
GO:0035295	tube development	6.10E-05
GO:0035239	tube morphogenesis	1.31E-04
GO:0048706	embryonic skeletal system development	2.16E-03
GO:0060562	epithelial tube morphogenesis	8.11E-03
GO:0060348	bone development	1.54E-02
GO:0002053	positive regulation of mesenchymal cell proliferation	1.68E-02
GO:0010464	regulation of mesenchymal cell proliferation	1.88E-02
GO:0048701	embryonic cranial skeleton morphogenesis	1.88E-02
GO:0048762	mesenchymal cell differentiation	2.23E-02
GO:0014031	mesenchymal cell development	2.23E-02
GO:0060485	mesenchyme development	2.35E-02
GO:0051216	cartilage development	5.73E-02
GO:0014032	neural crest cell development	5.78E-02
GO:0014033	neural crest cell differentiation	5.78E-02

Table 2. Gene Ontology Analysis of 200 Genes upregulated in $p75^{+}/HNK1^{+}$ cells relative to $PSA\text{-}NCAM^{+}$ cells

GO Accession	Gene Ontology (GO) Term	Corrected P Value
GO:0001501	skeletal system development	2.60E-10
GO:0007389	pattern specification process	4.97E-08
GO:0035295	tube development	2.29E-07
GO:0035239	tube morphogenesis	4.42E-07
GO:0042127	regulation of cell proliferation	5.40E-07
GO:0048706	embryonic skeletal system development	7.94E-07
GO:0008284	positive regulation of cell proliferation	1.23E-05
GO:0048705	skeletal system morphogenesis	1.35E-05
GO:0060485	mesenchyme development	1.47E-04
GO:0048704	embryonic skeletal system morphogenesis	2.29E-04
GO:0060562	epithelial tube morphogenesis	4.88E-04
GO:0014031	mesenchymal cell development	1.52E-03
GO:0048762	mesenchymal cell differentiation	1.52E-03
GO:0014033	neural crest cell differentiation	4.00E-03
GO:0014032	neural crest cell development	4.00E-03
GO:0001843	neural tube closure	3.44E-02
GO:0060606	tube closure	3.44E-02
GO:0051216	cartilage development	3.56E-02
GO:0014020	primary neural tube formation	4.10E-02
GO:0001841	neural tube formation	5.79E-02

Table 3. Gene Ontology (GO) Analysis of 257 Genes upregulated in PSA-NCAM$^-$ cells relative to PSA-NCAM$^+$ cells

GO Accession	GO Term	Corrected P Value	Epithelial-Mesenchymal Transition (EMT)
GO:0001568	blood vessel development	6.69E-04	**EMT**
GO:0001944	vasculature development	8.06E-04	**EMT**
GO:0048514	blood vessel morphogenesis	3.62E-03	**EMT**
GO:0048010	vascular endothelial growth factor receptor signaling pathway	7.13E-03	**EMT**
GO:0018108	peptidyl-tyrosine phosphorylation	1.70E-02	**EMT**
GO:0030198	extracellular matrix organization	3.49E-02	**EMT**
GO:0043062	extracellular structure organization	4.43E-02	**EMT**
GO:0001525	angiogenesis	9.87E-02	**EMT**

Table 4. Gene Ontology (GO) Analysis of 200 Genes upregulated in $p75^{+}/HNK1^{+}$ cells relative to $PSA\text{-}NCAM^{+}$ cells

GO Accession	GO Term	Corrected P Value	Epithelial-Mesenchymal Transition (EMT)
GO:0030198	extracellular matrix organization	7.66E-07	**EMT**
GO:0043062	extracellular structure organization	4.32E-06	**EMT**
GO:0001568	blood vessel development	1.43E-04	**EMT**
GO:0001944	vasculature development	1.74E-04	**EMT**
GO:0001569	patterning of blood vessels	1.06E-03	**EMT**
GO:0048514	blood vessel morphogenesis	1.73E-02	**EMT**
GO:0001525	angiogenesis	5.69E-02	**EMT**
GO:0030334	regulation of cell migration	8.35E-02	**EMT**
GO:0014829	vascular smooth muscle contraction	8.45E-02	**EMT**

Table 5. Semi-quantitative PCR Primer Sequences

Name	Tm (℃)	Size	Sequence
FAM70A	59.3	238	CCA GGA CCC AGA ATG TGA CT
	57.3		ACA TAA TGG CAC CGG TTA GC
EVI1	57.3	206	CAC ATT CGC TCT CAG CAT GT
	55.3		ATT TGG GTT CTG CAA TCA GC
ZNF312	59.3	228	GCC TTC CAC CAG GTC TAC AA
	61.4		GGT ACA GGG AGG GAA GGA AG
LIX1	59.3	217	ATG AGT CAC TGC CAG CTC CT
	61.4		GTG GAG GCT ACT GCT TCC TG
RSPO3	57.3	184	GGC ATG AAG CAG ATT GGA GT
	55.3		GGC AAT TGT CAA GGC ACT TT
PLZF	61.4	152	CTA TGG GCG AGA GGA GAG TG
	57.3		TCA ATA CAG CGT CAG CCT TG
DACH1	57.6	208	GTG GAA AAC ACC CCT CAG AA
	57.9		CTT GTT CCA CAT TGC ACA CC
PLAGL1	59.1	234	GCC TCA GTC ACC TCA AAA GC
	57.7		CTT AAC CTG TGG GGC AAA GA
MMRN1	59.3	224	CAG GGA GCA TCA CTC AGA CA
	55.3		TTG AGG CCA TCT TCC ATT TC
NR2F1	59.4	194	ACA GGA ACT GTC CCA TCG AC
	60.0		GAT GTA GCC GGA CAG GTA GC
DMRT3	59.3	182	CTA CCC CAT CTC GTC TTC CA
	57.3		ACT GGC TTC TCG CCA AAG TA
OCT4	58.4	311	CGT TCT CTT TGG AAA GGT GTT C
	59.3		ACA CTC GGA CCA CGT CTT TC
NANOG	55.3	158	CAA AGG CAA ACA ACC CAC TT
	59.3		TCT GCT GGA GGC TGA GGT AT
REX1	59.8	145	TCA CAG TCC AGC AGG TGT TTG
	55.3		TCT TGT CTT TGC CCG TTT CT
GAPDH	57.4	452	ACC ACA GTC CAT GCC ATC AC
	57.4		TCC ACC ACC CTG TTG CTG TA

Table 6. Real-time PCR Primers Sequences

Name	Tm (℃)	Sequence
p75	57.9	TCA TCC CTG TCT ATT GCT CCA
	57.3	TGT TCT GCT TGC AGC TGT TC
AdipoQ	63.7	CAG GCC GTG ATG GCA GAG ATG
	62.4	GGT TTC ACC GAT GTC TCC CTT AG
AP2	57.3	TAA AGC TGC CAA CGT TAC CC
	58.8	AAG TCC CTG GCT AGG TGG A
ITGB1	62.4	GGA TTC TCC AGA AGG TGG TTT CG
(CD29)	59.8	TGC CAC CAA GTT TCC CAT CTC
CD44	62.1	CCA GAA GGA ACA GTG GTT TGG C
	62.1	ACT GTC CTC TGG GCT TGG TGT T
NT5E	62.1	AGTCCACTGGAGAGTTCCTGCA
(CD73)	62.1	TGAGAGGGTCATAACTGGGCAC
ENG	62.1	CGG TGG TCA ATA TCC TGT CGA G
(CD105)	62.1	AGG AAG TGT GGG CTG AGG TAG A
THY1	62.1	GAA GGT CCT CTA CTT ATC CGC C
(CD90)	62.1	TGA TGC CCT CAC ACT TGA CCA G
CDH1	62.4	GCC TCC TGA AAA GAG AGT GGA AG
	62.1	TGG CAG TGT CTC TCC AAA TCC G
CDH2	62.4	CCT CCA GAG TTT ACT GCC ATG AC
	62.1	GTA GGA TCT CCG CCA CTG ATT C
cMyc	63.7	CCT GGT GCT CCA TGA GGA GAC
	62.1	CAG ACT CTG ACC TTT TGC CAG G
C/EBPα	62.1	AGG AGG ATG AAG CCA AGC AGC T
	64.0	AGT GCG CGA TCT GGA ACT GCA G
PDGFRα	61.4	GAC TTT CGC CAA AGT GGA GGA G
	65.5	AGC CAC CGT GAG TTC AGA ACG C
Runx2	62.1	CCC AGT ATG AGA GTA GGT GTC C
	62.1	GGG TAA GAC TGG TCA TAG GAC C
Slug	55.2	TGG TTG CTT CAA GGA CAC AT
	56.7	GTT GCA GTG AGG GCA AGA A

Snail	59.8	GAG CTG CAG GAC TCT AAT CCA
	58.2	CGG TGG GGT TGA GGA TCT
Sox8	64.0	ACA ACG CCG AGC TCA GCA AGA C
	62.1	TCC TTC TTG TGC TGC ACG CGA A
Sox9	56.0	AAC GCC TTC ATG GTG TGG
	59.8	TCT CGC TCT CGT TCA GAA GTC
Twist1	62.1	GCC AGG TAC ATC GAC TTC CTC T
	64.0	TCC ATC CTC CAG ACC GAG AAG G
ST8SIA2	57.3	TAT CCT GAA GCA CCA CGT CA
	57.9	TTT GTT GGT CAG CCA GTA TCC
ST8SIA4	59.3	AGA ACT GAG GAG CAC CAG GA
	60.6	GCT ATT GAC AAG TGA CCG ACT CA
Vimentin	62.1	AGG CAA AGC AGG AGT CCA CTG A
	62.1	ATC TGG CGT TCC AGG GAC TCA T
β-Actin	57.3	GCT CTT TTC CAG CCT TCC TT
	57.3	CTT CTG CAT CCT GTC AGC AA

3. Removal of PSA from PSA-NCAM$^+$ Cells or Low-density Culture of PSA-NCAM$^+$ Cells Leads to Increased Neural Crest Cell Marker Expression

The data demonstrate that PSA-NCAM$^-$ cells from neural rosette cultures are highly positive for neural crest markers. Although previous studies have taken advantage of PSA-NCAM expression to enrich NPCs or identify neuronal cells, they did not acknowledge the relationship between PSA-NCAM expression and the neural crest lineage of cells.[10, 24-26] Based on a report suggesting PSA-NCAM involvement in the regulation of *p75* gene expression in subventricular zone-derived neurons,[27] I sought to examine the relationship between PSA-NCAM and p75$^+$ neural crest cell generation. No p75$^+$ neural crest cell was found in the PSA-NCAM$^+$ cell population (Figure 7A). However, unlike the glycerol control condition, p75$^+$ cells appeared after PSA-NCAM$^+$ cells were treated with endoneuraminidase-N (EndoN), an enzyme that specifically removes PSA from NCAM (Figure 7A-F). Conversely, treatment of PSA-NCAM$^-$ cells with either glycerol or EndoN did not alter the number of p75$^+$ cells (Figure 7G-L). Real-time RT-PCR analysis further confirmed that treatment of PSA-NCAM$^+$ cells with EndoN upregulated *p75* gene expression but did not enhance transcription of *ST8SIA2* and *ST8SIA4* genes encoding polysialyltransferases that are responsible for NCAM polysialylation (Figure 7M, N). Although removing PSA from PSA-NCAM$^+$ cells increased p75 expression, it did not affect the neural crest cell lineage-commitment process showing no significant differences in the expression levels of other NCSC-related genes (Figure 7O). These results may suggest that any observed increase of p75 expression in PSA-NCAM$^+$ cells after PSA removal was not due to NCSC lineage commitment; rather, the PSA moiety of the PSA-NCAM protein negatively

regulated *p75* gene expression, causing a lack of $p75^+$ neural crest cells in the PSA-$NCAM^+$ cell population. Thus, the data suggest an inverse relationship between PSA-NCAM and p75 during the neural induction process, thereby explaining why only PSA-$NCAM^-$ cells are highly positive for p75.

The study also continued the investigation to determine whether that prolonged culture of positive or negative population leads to gradual accumulation or depletion of the NCSC population. Upon prolonged passaging of PSA-$NCAM^-$ cells, No morphological change was observed indicating the presence of neuroepithelial cells in the culture population (data not shown). However, the appearance of cells that resemble PSA-$NCAM^-$ cells in the positive culture population was noted and it was noticed that the rate of NCSCs appearance increased based on the degree of confluence. Thus, it was speculated that a cell density-dependent regulation might occur in the PSA-$NCAM^+$ culture system. To investigate this further, transcriptional changes of PSA-$NCAM^+$ cells (passage 4-8) in different density populations (cells/cm^2) were examined. Notably, expression levels of neural rosette-specific marker genes such as *PLZF* and *DASH1* as well as neuroepithelial marker genes such as *PAX6* and *SOX1*, showed significant decreases in the lowest density of PSA-$NCAM^+$ cells (Figure 8A-D). Conversely, neural crest cell marker genes such as *AP2* and *p75* showed significant increases in the lowest density (Figure 8E, F). At a high density of PSA-$NCAM^+$ cells, 2.5×10^6 cells/cm^2, only $SOX1^+$ cells were observed with no appearance of $AP2^+$ cells. However, at a lowest density of PSA-$NCAM^+$ cells, 1.0×10^6 cells/cm^2, scattered $AP2^+$ cells were noted around $SOX1^+$ cells (Figure 8G). These data demonstrate that prolonged passaging of PSA-$NCAM^+$ cells at a high density is required to maintain neuroepithelial cell purity while minimizing the possible appearance of PSA-$NCAM^-$ cells.

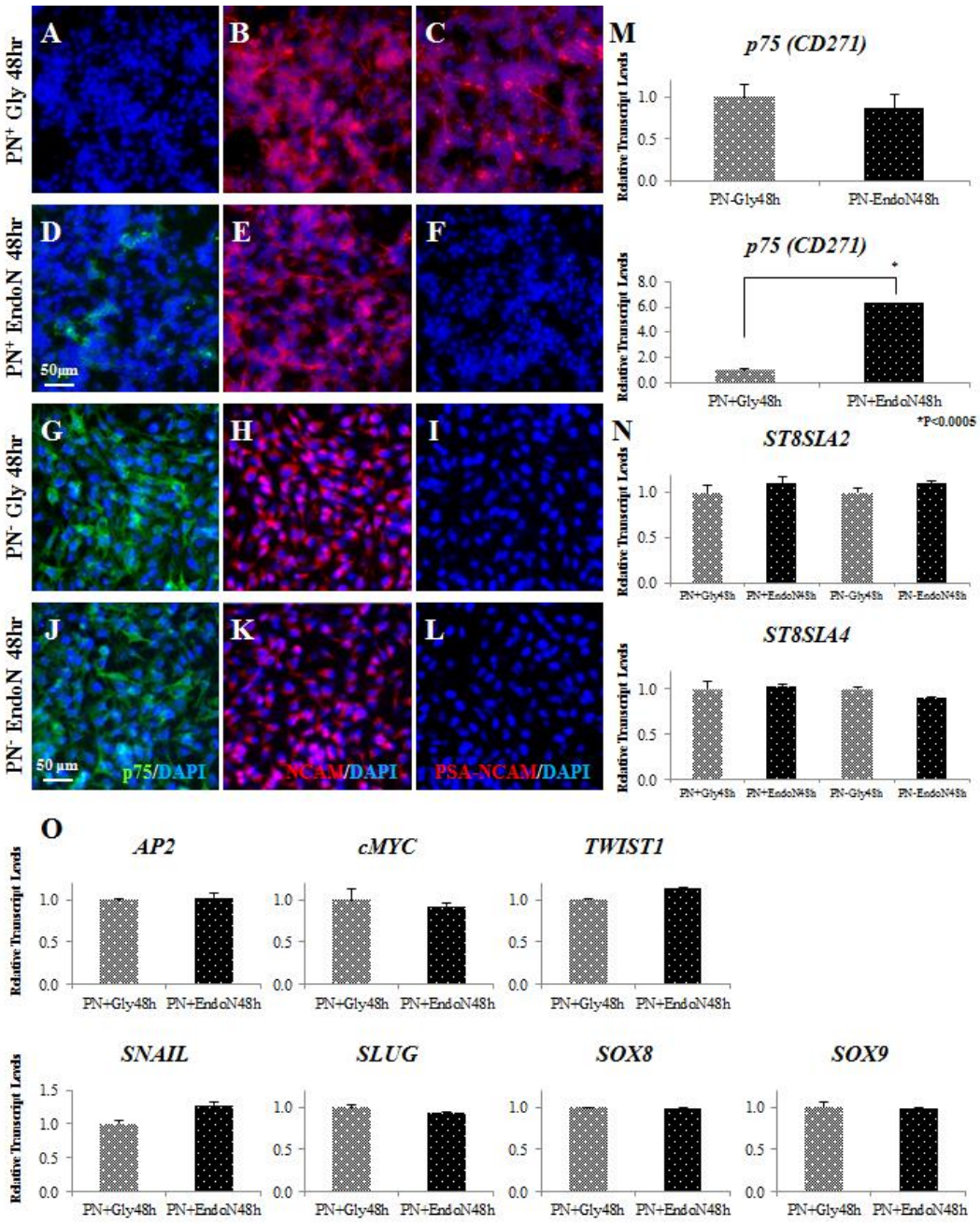

Figure7: Exposure to EndoN reveals an inverse relationship between PSA-NCAM and p75 in PSA-NCAM$^+$ cells. (A-C) PSA-NCAM$^+$ cells (PN$^+$) were treated with glycerol (Gly) for 48 hr. They showed no p75 expression but maintained NCAM and PSA-NCAM expression. (D-F) Endoneuraminidase-N (EndoN) treatment for 48 hr induced p75 expression in PN$^+$ cells but eliminated PSA-NCAM expression. (G-L) Neither Gly nor EndoN treatment affected p75 or PSA-NCAM expression in PSA-NCAM cells (PN$^-$). (M) Unlike PN$^-$ cells, 48-hr EndoN treatment increased *p75* expression in PN$^+$ cells compared to 48-hr Gly treatment when measured with real-time RT-PCR (*, $P < 0.0005$, Student's *t*-test, Mean ± SEM, n = 3 independent experiments). (N) *ST8SIA2* and *ST8SIA4* showed no expression change despite the treatment of Gly and EndoN in both PN$^+$ and PN$^-$ cells (Mean ± SEM, n = 3 independent experiments). (O) Transcripts related to neural crest cell identity showed no significant expression level changes despite the treatment of EndoN for 48hr in PN$^+$ cells (Mean ± SEM, n = 3 independent experiments).

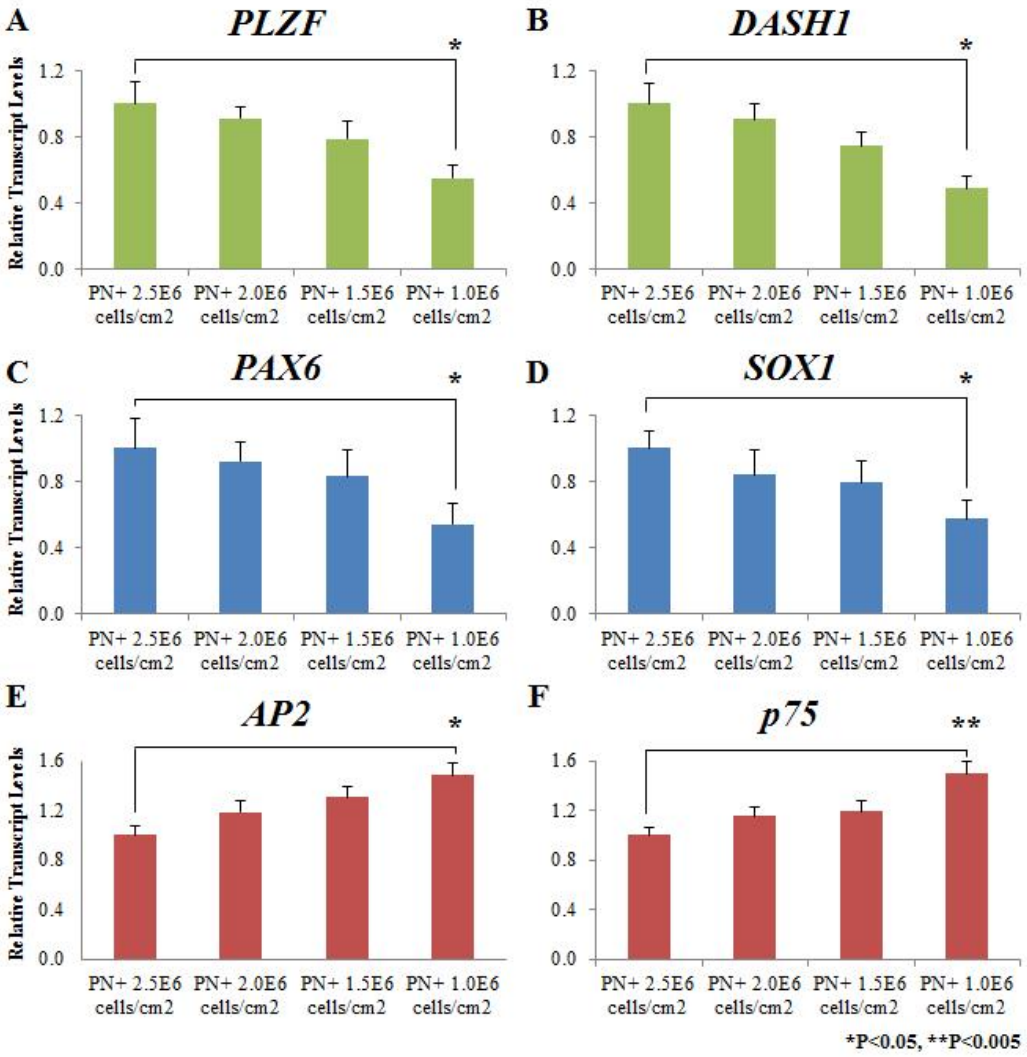

Figure 8: Prolonged culture of PSA-NCAM$^+$ cells increases neural crest cell marker gene expression in low densities. (A-F) Real-time RT-PCR to determine the changes in expression levels of rosette-specific, neuroepithelial, and neural crest cell marker genes in a density-gradient manner. Rosette-specific marker genes, *PLZF* and *DASH1* (A, B) and neuroepithelial marker genes, *PAX6* and *SOX1* (C, D) showed a significant decrease in the lowest density of PSA-NCAM$^+$ (PN$^+$) cells when compared with the highest density. Neural crest cell marker genes, *AP2* and *p75* (E, F), however, showed a significant increase in the lowest density of PN$^+$ cells when compared with the highest density (*, $P < 0.05$; **, $P < 0.005$, Student's *t*-test, Mean ± SEM, n = 3 independent experiments). (G) At a high density of PN$^+$ cells, 2.5×10^6 cells/cm^2, only SOX1$^+$ cells were observed with no appearance of AP2$^+$ cells. However, at a lowest density of PN$^+$ cells, 1.0×10^6 cells/cm^2, AP2$^+$ cells were observed peripheral to SOX1$^+$ cells.

4. PSA-NCAM$^-$ Cells Possess the Multilineage Differentiation Capacity of NCSCs

The neural crest is a multipotent population that originates from the dorsal region of the neural tube. NCSCs are multipotent, and can differentiate into both ectodermal and mesodermal tissue lineages.[14] To characterize the *in vitro* functionality of PSA-NCAM$^-$ cells, I promoted the differentiation of PSA-NCAM$^-$ cells into cells with a neural crest origin.[20] Prior to inducing the multilineage differentiation of PSA-NCAM$^-$ cells, It was ensured that there were no contaminating endodermal or mesodermal lineage cells. Neuroectoderm specified embryoid bodies (EBs) showed no contamination of endo- and mesodermal lineage cells prior to the PSA-NCAM-targeted sorting (Figure 9A, B). Thus, PSA-NCAM$^-$-derived mesodermal lineage cells during multilineage differentiation are solely dependent on PSA-NCAM$^-$ cell potency.

To examine whether PSA-NCAM$^-$ cells have the capacity to produce mesenchymal progenitors (MPs) mimicking neural crest development in vertebrates,[28-30] PSA-NCAM$^-$ cells were spontaneously differentiated by adding 10% fetal bovine serum (FBS) to the growth medium. Morphological changes were observed from day 4, and MPs appeared at day 14 (Figure 10A, B). Flow cytometry analysis at day 20 revealed the loss of p75 positivity in PSA-NCAM$^-$ cell-derived MPs, whereas mesenchymal markers such as CD44, CD29, CD73, CD105, and CD90 were detected (Figure 10C). To compare the ability to differentiate into mesenchymal lineages between PSA-NCAM$^-$ cells and p75$^+$/HNK1$^+$ cells, real-time RT-PCR analysis was performed targeting EMT marker genes such as *SNAIL*, *SLUG*, *TWIST1*, and *VIMENTIN* as well as mesenchymal marker genes such as *CD29*, *CD44*, *CD73*, *CD90*, *CD105*, and *PDGFRα*. When the expression levels of both cell

types exposed to 10% FBS were compared every 4 days for up to 32 days, no significant differences were observed (Figure 11A). The data suggest that both types of cells are capable of differentiating into MPs. PSA-NCAM$^+$ cells, on the other hand, failed to differentiate into mesenchymal lineages showing no significant increase in the expression levels of either EMT or mesenchymal markers but showed a decrease in cell viability when exposed to 10% FBS (Figure 12A-E).

It was also determined that the MPs differentiated from PSA-NCAM$^-$ cells retained chondrogenic, osteogenic, and adipogenic differentiation potentials (Figure 10D-F). The multipotency of NCSCs also includes differentiation into neurons that comprise the PNS. Late-passaged PSA-NCAM$^-$ cells (p6-8) were induced to differentiate into PERIPHERIN$^+$ neurons via neuronal induction.[18] NESTIN$^+$/PSA-NCAM$^-$ cells slowly lost their neural precursor characteristics and differentiated into TuJ1$^+$ neuronal cells (Figure 10G). PERIPHERIN$^+$ and TuJ1$^+$ PNS neurons were obtained on day 14 (Figure 10H). Finally, PSA-NCAM$^-$ cells could also differentiate into smooth muscle actin α (SMAα) and CALPONIN$^+$ smooth muscle cells (Figure 10I, J), further demonstrating the multipotentiality of PSA-NCAM$^-$ cells *in vitro*. Acquisition of mesenchymal features was also observed in iPSC-derived PSA-NCAM$^-$ cells (Figure 13A), and these cells could also differentiate into SMAα$^+$ and CALPONIN$^+$ cells (Figure 13B, C). Similar to bona fide neural crest cells *in vivo*, the data confirmed the multipotent behavior of PSA-NCAM$^-$ cells.

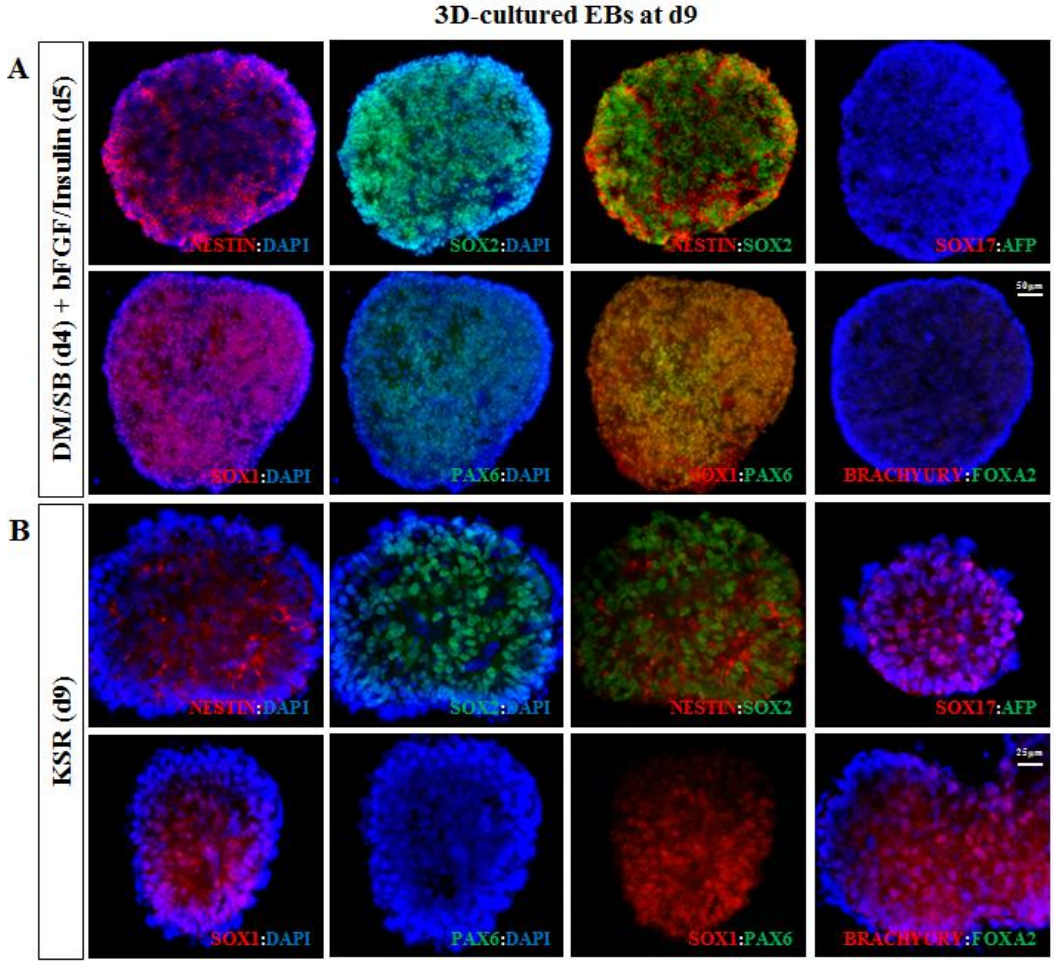

Figure 9: Lineage characterization of neuroectoderm specified EBs. (A) hESCs that had been induced to neuroectoderm via dual-SMAD inhibition and through bFGF and insulin showed no positivity of endo- or mesodermal markers, whereas strong expression of neuroepithelial markers (NESTIN, SOX2, SOX1, and PAX6) was detected. (B) In contrast, spontaneously differentiated hESCs in the form of EBs contained NESTIN, SOX2, and $SOX1^{+}$ neuroectoderm, $BRACHURY^{+}$ mesoderm, and $SOX17^{+}$ endoderm.

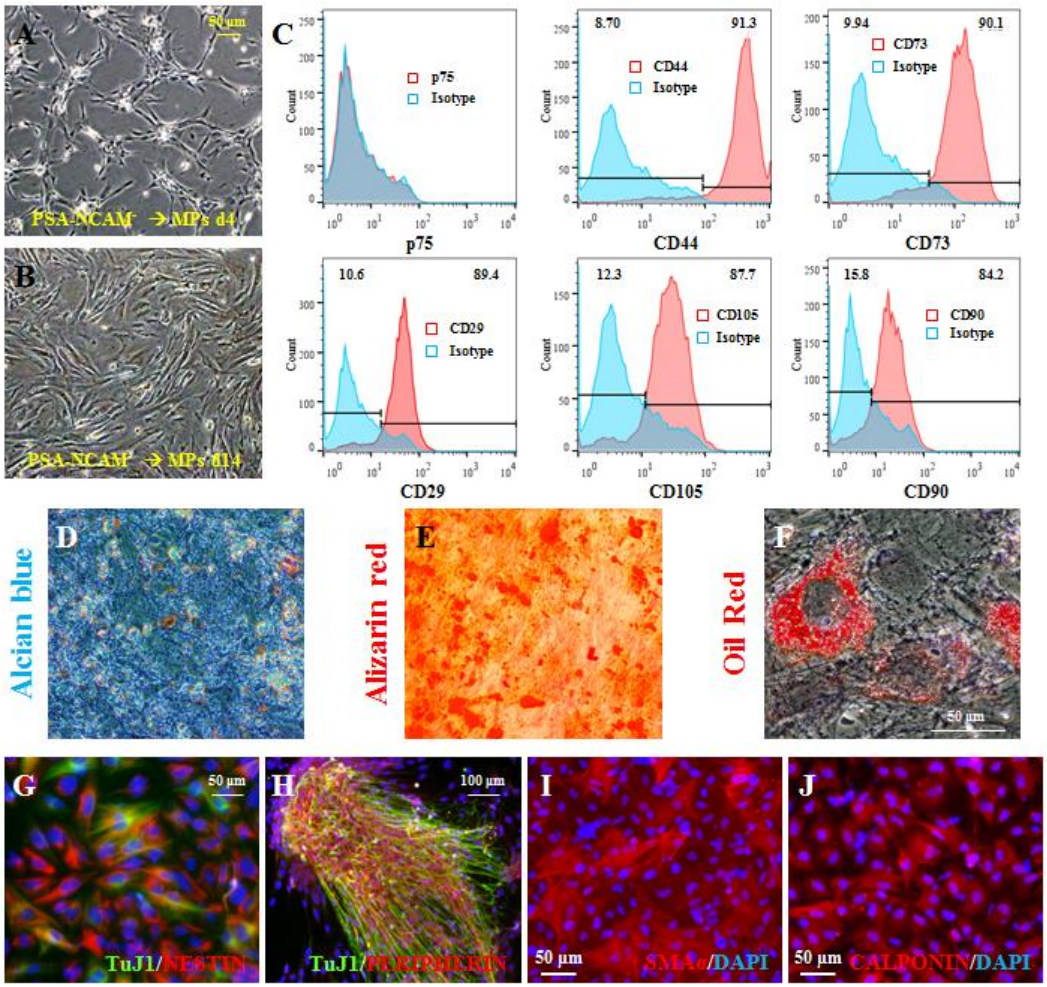

Figure 10: PSA-NCAM$^-$ cells can be induced to differentiate into multilineages of NCSCs. (A and B) Bright-field images of mesenchymal progenitors (MPs) differentiated from PSA-NCAM$^-$ (at d4 and d14). (C) Loss of p75$^+$ expression in PSA-NCAM$^-$ cell-derived MPs. Strong expressions of mesenchymal cell markers were detected, including CD44, CD29, CD73, CD105, and CD90. (D-F) Generated MPs were further differentiated into the mesenchymal lineages including, Alcian blue-stained chondrocytes (D), Alizarin red-stained osteocytes (E), and Oil red O-stained adipocytes with oil droplets (red) (F). (G and H) PSA-NCAM$^-$ cells were induced to differentiate into PERIPHERIN$^+$ neuronal cells. NESTIN$^+$ PSA-NCAM$^-$ cells were slowly lost but gained TuJ1- and PERIPHERIN-positivity. (I and J) SMAα^+ and CALPONIN$^+$ smooth muscle cells were also obtained.

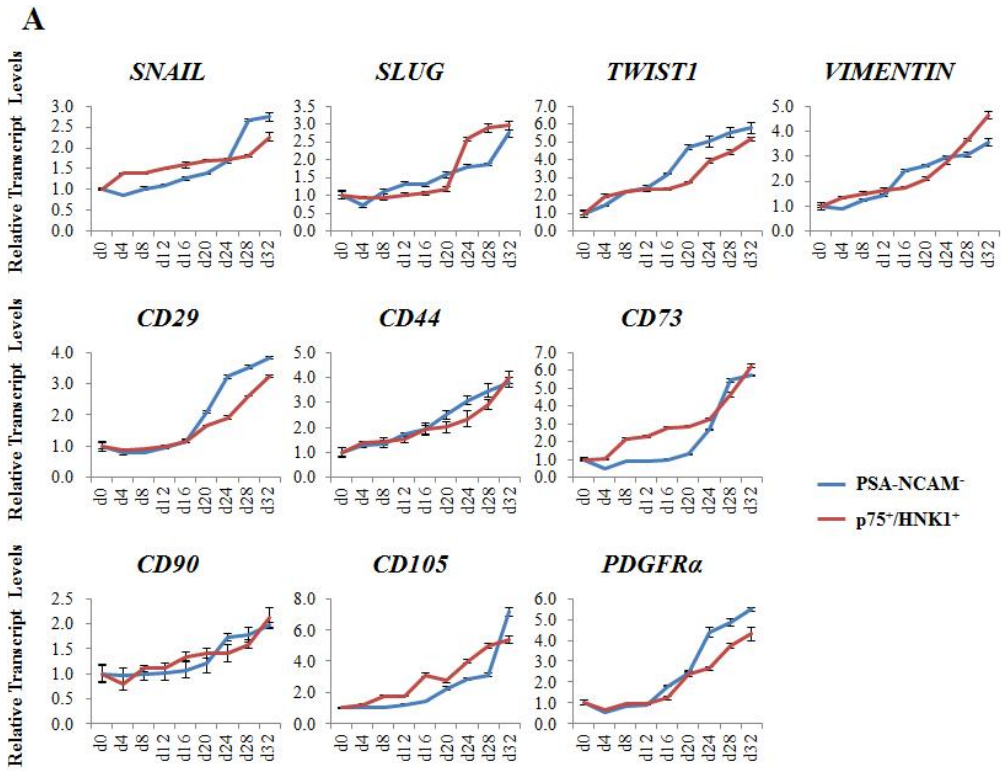

Figure 11: Comparison of the ability to differentiate into mesenchymal lineages between PSA-NCAM$^-$ cells and p75$^+$/HNK1$^+$ cells. (A) Real-time RT-PCR analysis targeting EMT marker genes such as *SNAIL*, *SLUG*, *TWIST1*, and *VIMENTIN* as well as mesenchymal marker genes such as *CD29*, *CD44*, *CD73*, *CD90*, *CD105*, and *PDGFRα*. The expression levels of both cell types that were exposed to 10% FBS were compared every 4 days for up to 32 days (Student's *t*-test, Mean ± SEM, n = 3 independent experiments).

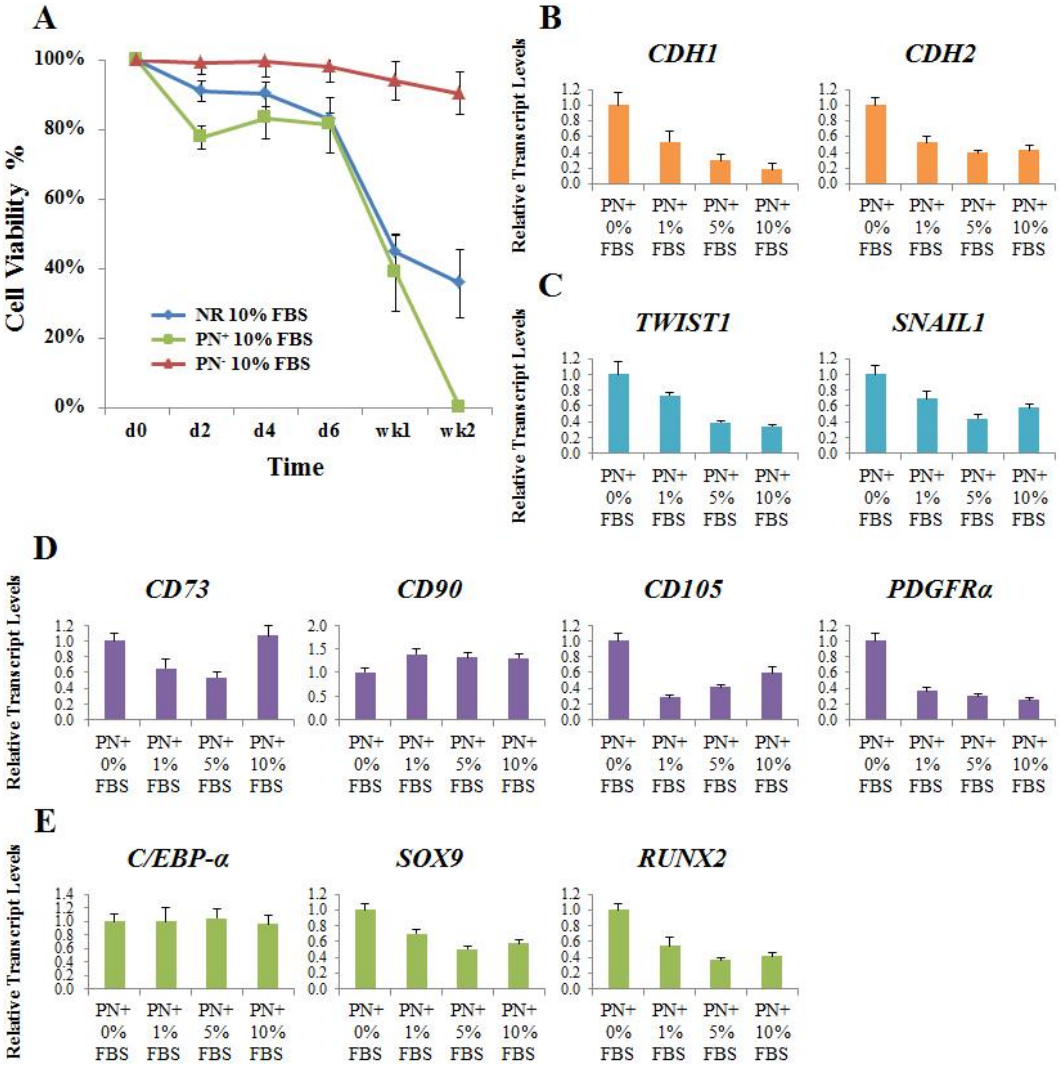

Figure 12: No multilineage differentiation capacity of PSA-NCAM$^+$ cells. (A) Trypan blue exclusion assay showed that 10% FBS exposure in a time-dependent manner decreased cell viability in neural rosettes (NR) and PSA-NCAM$^+$ (PN$^+$) cells starting from day 6, while PSA-NCAM$^-$ (PN$^-$) cells maintained their viability for up to 2 wk (Mean ± SD, n = 3 independent experiments). (B-D) Real-time RT-PCR analysis targeting cadherin genes, EMT and mesenchymal marker genes after the FBS treatment in a dose-dependent manner. PN$^+$ cells were exposed to different concentrations of FBS for 6 days and showed decreased expression levels of *CDH1* (E-cadherin) and *CDH2* (N-cadherin) (B). Reduced expression levels of EMT marker genes such as *TWIST1*, and *SNAIL1* were observed (C). FBS exposure did not induce significant difference in the expression levels of mesenchymal marker genes *CD73*, *CD90*, *CD105*, and *PDGFRα* (D) (Student's *t*-test, Mean ± SEM, n = 3 independent experiments). (E) PN$^+$ cells exposed to FBS did not exhibit any significant transcriptional activity for *C/EBP-α* (pre-adipocyte marker gene), *SOX9* (pre-chondrocyte marker gene), or *RUNX2* (osteoprogenitor marker gene) (Student's *t*-test, Mean ± SEM, n = 3 independent experiments).

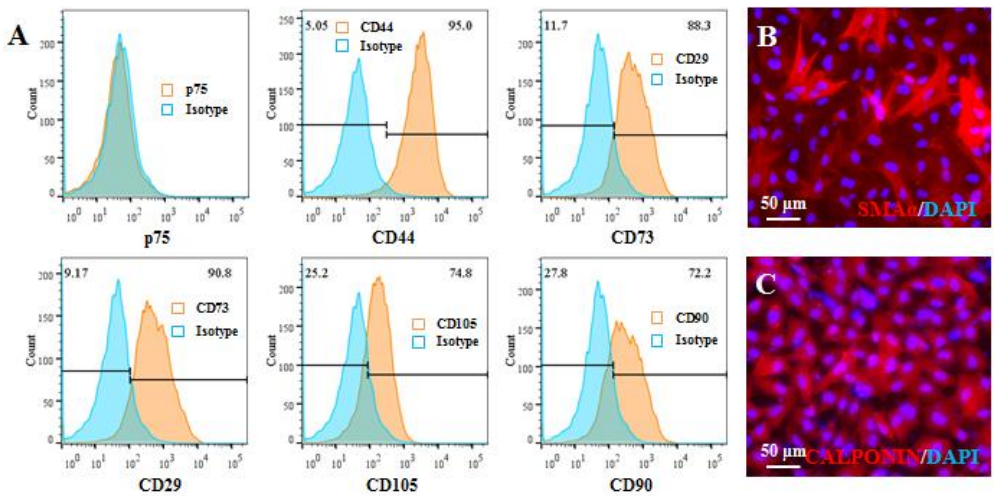

Figure 13: PSA-NCAM$^-$ cells derived from WT-iPSCEpi3 also show multilineage differentiation capacity of NCSCs. (A) WT-iPSCEpi3-derived PSA-NCAM$^-$ cells were induced to differentiate into MPs expressing CD44, CD29, CD73, CD105, and CD90 while losing the p75 expression. Plots shown are representative of results from three different WT-iPSCEpi3-PSA-NCAM$^-$-derived MP cultures (n = 3). (B, C) iPSC-derived PSA-NCAM$^-$ cells could also differentiate into SMAα$^+$ and CALPONIN$^+$ cells.

5. Tumors of Mesodermal Lineage, Pigmented Cells and PERIPHERIN$^+$ Grafts Derived from PSA-NCAM$^-$ Cells

To characterize the cellular behavior of heterogeneous neural rosettes *in vivo*, transplantations in adult rat brains were performed. At 10 wk post-transplantation, a rosette-rich neural overgrowth (Figure 14A-C) and nonneuroectodermal origin grafts were observed[31] such as a runt-related transcription factor 2 (RUNX2)$^+$ structure (Figure 14D, E). Rosette-forming neural overgrowth was identified in all transplanted animals (n = 8) while nonneuroectodermal structures with mesodermal lineages (referred to here as tumors) were developed in all but one of the animals (n = 7/8, 88%) (Figure 14F).

Previous studies which reported tumor formation following cell engraftment[8-10, 12] and the fact that melanocytes, chondrocytes, and smooth muscle cells could be derived from NCSCs prompted us to examine whether PSA-NCAM$^-$ cells play a tumorigenic role when neural rosettes are used as a transplantation material. PSA-NCAM$^-$ cells were mixed with PSA-NCAM$^+$ cells at specific ratios and transplanted into the rat brain as follows: 100% PSA-NCAM$^-$ cells; 75% PSA-NCAM$^-$ cells/25% PSA-NCAM$^+$ cells; 25% PSA-NCAM$^-$ cells/75% PSA-NCAM$^+$ cells; and 100% PSA-NCAM$^+$ cells. Overall, 82%, 75%, and 57% of rats grafted with 100%, 75%, and 25% PSA-NCAM$^-$ cells developed tumors, respectively (Figure 14G). By contrast, neither tumor formation nor neural overgrowth was detected in animals grafted with 100% PSA-NCAM$^+$ cells. The grafts formed by the PSA-NCAM$^-$ cells also contained PERIPHERIN$^+$ cells and showed pigmentation as well as cyst formation (Figure 14H, I). Identified tumors were consisted of mesodermal lineage derivatives, such as RUNX2-expressing bone and SMAα-expressing smooth muscle tissues (Figure 14J, K). Representative

hematoxylin and eosin (H&E) staining of rat brains revealed various mesodermal lineages but showed no endodermal lineage grafting (Figure 14L). While the 100% PSA-NCAM^{+} cell grafts showed no sign of neural overgrowth or tumor formation (Figure 14M), the groups with PSA-NCAM^{-} cells included in the grafts showed smooth muscle tissue, cyst formation, pigmentation, and pre-chondrogenic tissue (Figure 14N-Q).

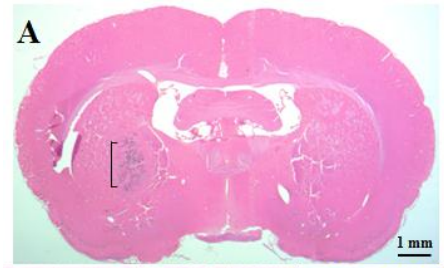

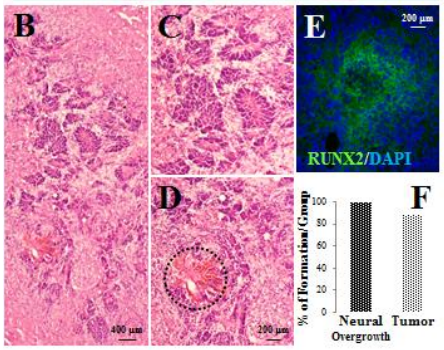

G Frequency of Tumor and Lineages of Grafted Cells Derived from PSA-NCAM$^{+/-}$

Cell Type Injected		Tumor Formation	Endoderm	Mesoderm	Ectoderm
Neural Rosette		7/8 (88)	0/8 (0)	7/8 (88)	8/8 (100)
100%	PSA-NCAM$^-$	9/11 (82)	0/11 (0)	9/11 (82)	11/11 (100)
75% 25%	PSA-NCAM$^-$ PSA-NCAM$^+$	6/8 (75)	0/8 (0)	6/8 (75)	8/8 (100)
25% 75%	PSA-NCAM$^-$ PSA-NCAM$^+$	4/7 (57)	0/7 (0)	4/7 (57)	7/7 (100)
100%	PSA-NCAM$^+$	0/11 (0)	0/11 (0)	0/11 (0)	11/11 (100)

H Frequency of Unwanted Biological Effect (%)

Cell Type Injected		PERIPHERIN$^+$ Graft	Pigmentation	Graft Rejection (Cyst Formation)
Neural Rosette		2/8 (25)	2/8 (25)	-
100%	PSA-NCAM$^-$	5/11 (45)	1/11 (9)	1/11 (9)
75% 25%	PSA-NCAM$^-$ PSA-NCAM$^+$	3/8 (37.5)	0/8 (0)	1/8 (12.5)
25% 75%	PSA-NCAM$^-$ PSA-NCAM$^+$	2/7 (28.6)	0/7 (0)	-
100%	PSA-NCAM$^+$	0/11 (0)	0/11 (0)	-

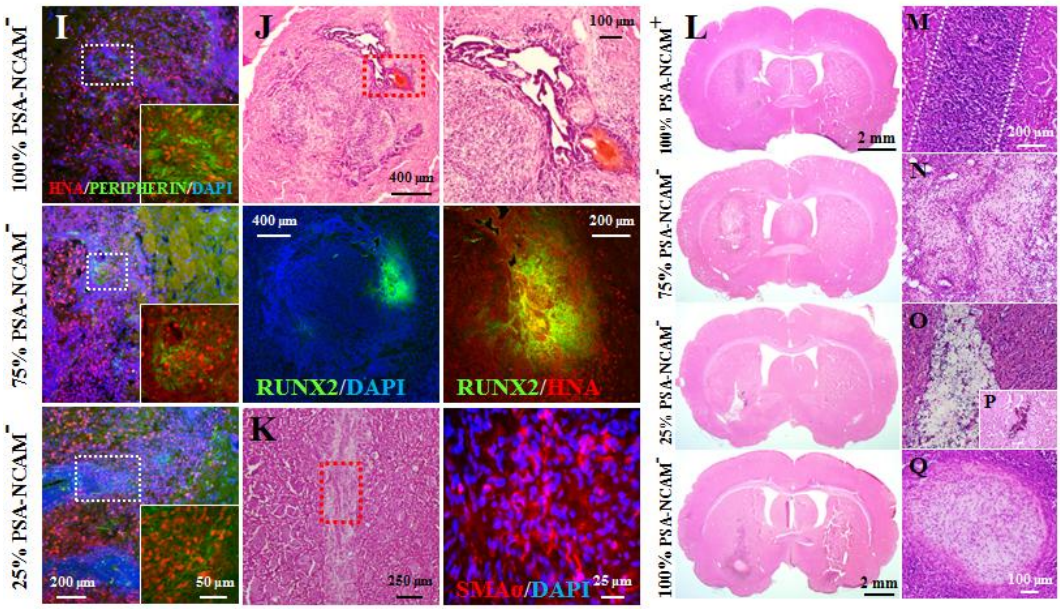

Figure 14: Tumors of mesodermal lineage and PERIPHERIN^{+} grafts can be derived from PSA-NCAM^{-} cells. (A-C) Representative H&E-stained neural rosette graft showing neural overgrowth. (D and E) Structures of nonneuroectodermal origin such as RUNX2^{+} graft. (F) Neural overgrowth and tumor formation detected at rates of 100% and 88%, respectively from neural rosette grafts. (G) Summary of tumor formation and cell lineages derived from PSA-NCAM$^{+/-}$ grafts. Regardless of tumor formation, lineages were identified based on apparent phenotypes. (H) The frequencies of PERIPHERIN^{+}, pigmented graft detection, and cyst formation. (I) HNA^{+}/PERIPHERIN^{+} in grafts with PSA-NCAM^{-} cells. (J) H&E staining and immunofluorescent histochemistry analysis showing RUNX2^{+}/HNA^{+} bone tissue in PSA-NCAM^{-} grafts. (K) SMAα^{+} smooth muscle tissue detected in PSA-NCAM^{-} grafts. (L) Representative H&E-stained coronal images revealing tumors of mesodermal lineage from PSA-NCAM^{-} grafts (bottom three images) unlike the 100% PSA-NCAM^{+} graft (top image). (M) PSA-NCAM^{+} cell graft showed no sign of neural overgrowth or tumor formation. (N) The groups with PSA-NCAM^{-} cell grafts showed smooth muscle tissue. (O, P) Cyst formation and pigmentation observed in the groups with PSA-NCAM^{-} cell grafts. (Q) Pre-chondrogenic tissue formation observed in the groups with PSA-NCAM^{-} cell grafts.

IV. DISCUSSION

In this study, the cause of mesodermal tumor development after CNS transplantation of neural rosette-NPCs was analyzed. The results demonstrate that the multipotent characteristics of NCSCs among the neural rosette populations are responsible for mesodermal tumor formation, PERIPHERIN$^+$ grafts, and the presence of pigmented cells. Thus, identifying surface markers such as PSA-NCAM that could distinguish between NPCs with CNS characteristics and NCSCs from neural rosette cell culture populations could reduce the tumorigenic potential of hPSC-derived NPCs.

Previously it was demonstrated that targeting PSA-NCAM$^+$ cells via MACS from neural rosettes obtained through dual-SMAD inhibition-induced neuralization could enrich NPCs up to 85% SOX1$^+$ cells.[12] When these PSA-NCAM$^+$ sorted cells were further analyzed with FACS to confirm the MACS results, 93% of cells were PSA-NCAM$^+$. Meanwhile, the current study involved the expansion of neural rosettes obtained through the same method to produce a large number of cells for *in vivo* transplantation. According to the data (n = 4), the total neural rosette culture population after 7 days of expansion was 79% PSA-NCAM$^+$ cells and 21% PSA-NCAM$^-$ cells (Figure 1L).

Despite efforts to increase the efficiency of neural induction to achieve full neural conversion of hPSCs, the current dual-SMAD inhibition-induced neuralization method yields >80% PAX6$^+$ and 82% HES5$^+$ cells[32] with >90% of total colonies containing neural rosettes.[11] Although the ultimate goal would be to prevent NCSC development during the neural induction of hPSCs, this is challenging since NCSCs and SOX1$^+$/PAX6$^+$ neuroepithelial cells share the same major developmental signals including bone morphogenetic proteins (BMP), Wnt, fibroblast growth factor (FGF), and Notch signaling pathways.[33] As a result, an elaborate differentiation

method was required to increase the purity of $SOX1^+/PAX6^+$ neuroepithelial cells while suppressing NCSC development. The first approach was employed in a previous study and achieved a decrease of $p75^+$ after treatment with FGF and BMP antagonists.[13] Though it may be possible to obtain >80% $SOX1^+/PAX6^+$ neuroepithelial cells via the initial isolation of neural rosettes, I would expect that the purity inevitably decreases during expansion to produce a large number of cells without any targeted cell sorting or antagonist treatment. Based on this information, I have concluded that 21% PSA-$NCAM^-$ cells in the neural rosette culture population was a reasonable proportion.

PSA-NCAM-targeted cell sorting from neural rosettes allowed an isolation of NCSC populations. Compared to the previously defined hPSC-derived NCSCs, $p75^+/HNK1^+$ cells, PSA-$NCAM^-$ cells exhibited similar molecular characteristics and multipotentiality, i.e., both were able to generate ectodermal and mesodermal lineages. The study also identified an inverse relationship between PSA from NCAM and p75 in PSA-$NCAM^+$ cells. Removal of PSA from PSA-$NCAM^+$ cells with EndoN led to increased expression of the neural crest marker, p75, which explains enrichment of $p75^+$ cells in PSA-$NCAM^-$ populations (Figure 7). Though removing PSA from PSA-$NCAM^+$ cells showed no significant differences in the expression levels of NCSC-related genes other than *p75*, a hasty conclusion should not be made to exclude a possible role of PSA in NCSC lineage determination. Since the study targeted the removal of existing PSA from PSA-$NCAM^+$ cells in a short period of time, a loss-of-function study that acquires insights of protein function should be further considered to determine a role of PSA in NCSC lineage determination during the neural induction process.

Subsequently to PSA-NCAM-targeted cell sorting, in order to benefit from highly enriched PSA-$NCAM^+$ NPCs while shielded from PSA-

NCAM$^-$ NCSCs, it is important to understand whether gradual accumulation or depletion of PSA-NCAM$^-$ NCSCs occurs in the PSA-NCAM$^+$ culture population upon prolonged passaging. I determined that a cell density-dependent regulation took place in the PSA-NCAM$^+$ culture system and the rate of NCSC appearance increased when the degree of confluence of positive cells decreased (Figure 8). The data demonstrate that prolonged passaging of PSA-NCAM$^+$ cells at a high density is required to maintain neuroepithelial cell purity while minimizing the possible appearance of PSA-NCAM$^-$ cells. Though it has been determined that NCSCs originate from the border of neural and epidermal ectoderm based on "a long-standing interpretation" of developmental studies, it is still not clear whether NCSCs are induced or self-differentiated. If NCSCs are induced hypothetically, questions still remain whether their induction separates from, is part of, or occurs subsequent to the neural induction process of embryo.[34] Thus, I cannot yet conclude whether appeared PSA-NCAM$^-$ cells in a low density of PSA-NCAM$^+$ cells were self-differentiated or induced from PSA-NCAM$^+$ cells at this point.

Previous studies targeted remaining PSCs in cell cultures in attempts to deplete tumor-initiating cells.[35, 36] While such strategies were successful in removing PSCs, targeting PSCs alone was insufficient to completely eliminate tumorigenic potential of NPCs. Notably, the data indicate that isolated PSA-NCAM$^-$ cells play a significant role in mesodermal tumor development in the adult rat brain. The detection of mesodermal derivatives, PERIPHERIN$^+$ cells, and pigmented tissues in grafts of PSA-NCAM$^-$ cells suggested that tumorigenesis after neural rosette engraftment was caused by NCSCs that comprise the PSA-NCAM$^-$ cell population. the results demonstrate that PSA-NCAM$^-$ NCSCs can be a critical target for tumor prevention in hPSC-derived-NPC-based therapy and suggest that removal of

PSA-NCAM^{-} cells would completely eliminate the tumorigenic potential originating from NCSCs following transplantation of NPCs into the CNS.

V. CONCLUSION

Human pluripotent stem cell (hPSC)-derived neural precursor cells (NPCs) are self-renewing multipotent cells which hold promise for treatments of degenerative diseases and tissue damages. However, such characteristics of hPSC-derived NPCs bring inevitable risk factors to their clinical applications. Most efforts to eliminate risk factors of tumor formation have been focused on excluding residual pluripotent cells from donor cells before transplantation. Despite many efforts, hPSC-derived NPCs have repeatedly resulted in tumor formation when transplanted in the central nervous system (CNS) in animal models. During the early neural induction process to generate NPCs from hPSCs, the emergence of multipotent neural crest stem cells (NCSCs) has been less explored. Here, I show that multipotent polysialic acid-neural cell adhesion molecule (PSA-NCAM)-negative cells NCSCs with capacity to differentiate into both ectodermal and mesodermal lineages are responsible for mesodermal tumor formation *in vivo* and the formation of PERIPHERIN^{+} grafts in the CNS region. These results suggest that removal of PSA-NCAM^{-} cells from hPSC-derived NPCs eliminates the risk factor of tumor formation caused by NCSCs.

REFERENCES

1. Conti, L., and Cattaneo, E. (2010). Neural stem cell systems: physiological players or *in vitro* entities? Nat. Rev. Neurosci. 11, 176–187.

2. Chambers, S.M., Fasano, C.A., Papapetrou, E.P., Tomishima, M., Sadelain, M., and Studer, L. (2009). Highly efficient neural conversion of human ES and iPS cells by dual inhibition of SMAD signaling. Nat. Biotechnol. 27, 275–280.

3. Elkabetz, Y., Panagiotakos, G., Al Shamy, G., Socci, N.D., Tabar, V., and Studer, L. (2008). Human ES cell-derived neural rosettes reveal a functionally distinct early neural stem cell stage. Genes Dev. 22, 152–165.

4. Koch, P., Opitz, T., Steinbeck, J.A., Ladewig, J., and Brustle, O. (2009). A rosette-type, self-renewing human ES cell-derived neural stem cell with potential for *in vitro* instruction and synaptic integration. Proc. Natl. Acad. Sci. USA 106, 3225–3230.

5. Kirkeby, A., Grealish, S., Wolf, D.A., Nelander, J., Wood, J., Lundblad, M., et al. (2012). Generation of regionally specified neural progenitors and functional neurons from human embryonic stem cells under defined conditions. Cell Rep. 1, 703–714.

6. Kriks, S., Shim, J.W., Piao, J., Ganat, Y.M., Wakeman, D.R., Xie, Z., Carrillo-Reid, L., Auyeung, G., Antonacci, C., Buch, A., et al. (2011). Dopamine neurons derived from human ES cells efficiently engraft in animal models of Parkinson's disease. Nature 480, 547–551.

7. Liu, Y., Weick, J.P., Liu, H., Krencik, R., Zhang, X., Ma, L., et al. (2013). Medial ganglionic eminence-like cells derived from human embryonic stem cells correct learning and memory deficits. Nat. Biotechnol. 31, 440–447.

8. Arnhold, S., Klein, H., Semkova, I., Addicks, K., and Schraermeyer, U. (2004). Neurally selected embryonic stem cells induce tumor formation after long-term survival following engraftment into the subretinal space. Invest. Ophthalmol. Vis. Sci. 45, 4251–4255.

9. Seminatore, C., Polentes, J., Ellman, D., Kozubenko, N., Itier, V., Tine, S., et al. (2010). The postischemic environment differentially impacts teratoma or tumor

formation after transplantation of human embryonic stem cell-derived neural progenitors. Stroke 41, 153–159.

10. Doi, D., Morizane, A., Kikuchi, T., Onoe, H., Hayashi, T., Kawasaki, T., et al. (2012). Prolonged maturation culture favors a reduction in the tumorigenicity and the dopaminergic function of human ESC-derived neural cells in a primate model of Parkinson's disease. Stem Cells 30, 935–945.

11. Kim, D.S., Lee, J.S., Leem, J.W., Huh, Y.J., Kim, J.Y., Kim, H.S., et al. (2010). Robust enhancement of neural differentiation from human ES and iPS cells regardless of their innate difference in differentiation propensity. Stem Cell Rev. 6, 270–281.

12. Kim, D.S., Lee, D.R., Kim, H.S., Yoo, J.E., Jung, S.J., Lim, B.Y., et al. (2012). Highly pure and expandable PSA-NCAM-positive neural precursors from human ESC and iPSC-derived neural rosettes. PloS ONE 7, e39715.

13. Lee, G., Kim, H., Elkabetz, Y., Al Shamy, G., Panagiotakos, G., Barberi, T., et al. (2007). Isolation and directed differentiation of neural crest stem cells derived from human embryonic stem cells. Nat. Biotechnol. 25, 1468–1475.

14. Le Douarin, N.M., and Dupin, E. (2003). Multipotentiality of the neural crest. Curr. Opin. Genet. Dev. 13, 529–536.

15. Knecht, A.K., and Bronner-Fraser, M. (2002). Induction of the neural crest: a multigene process. Nat. Rev. Genet. 3, 453–461.

16. Jang, J., Kang, H.C., Kim, H.S., Kim, J.Y., Huh, Y.J., Kim, D.S., et al. (2011). Induced pluripotent stem cell models from X-linked adrenoleukodystrophy patients. Ann. Neurol. 70, 402–409.

17. Lee, M.Y., and Lufkin, T. (2012). Development of the "Three-step MACS": a novel strategy for isolating rare cell populations in the absence of known cell surface markers from complex animal tissue. J. Biomol. Tech. 23, 69–77.

18. Lee, G., Chambers, S.M., Tomishima, M.J., and Studer, L. (2010). Derivation of neural crest cells from human pluripotent stem cells. Nat. Protoc. 5, 688–701.

19. Prasad, M.S., Sauka-Spengler, T., and LaBonne, C. (2012). Induction of the neural crest state: control of stem cell attributes by gene regulatory, post-transcriptional and epigenetic interactions. Dev. Biol. 366, 10–21.

20. Chimge, N.O., and Bayarsaihan, D. (2010). Generation of neural crest progenitors from human embryonic stem cells. J. Exp. Zool. B Mol. Dev. Evol. 314, 95–103.

21. Jiang, X., Gwye, Y., McKeown, S.J., Bronner-Fraser, M., Lutzko, C., and Lawlor, E.R. (2009). Isolation and characterization of neural crest stem cells derived from *in vitro*-differentiated human embryonic stem cells. Stem Cells Dev. 18, 1059–1070.

22. Kreitzer, F.R., Salomonis, N., Sheehan, A., Huang, M., Park, J.S., Spindler, M.J., et al. (2013). A robust method to derive functional neural crest cells from human pluripotent stem cells. Am. J. Stem Cells 2, 119–131.

23. Menendez, L., Yatskievych, T.A., Antin, P.B., and Dalton, S. (2011). Wnt signaling and a Smad pathway blockade direct the differentiation of human pluripotent stem cells to multipotent neural crest cells. Proc. Natl. Acad. Sci. USA 108, 19240–19245.

24. Barral, S., Ecklebe, J., Tomiuk, S., Tiveron, M.C., Desoeuvre, A., Eckardt, D., et al. (2013). Efficient neuronal *in vitro* and *in vivo* differentiation after immunomagnetic purification of mESC derived neuronal precursors. Stem Cell Res. 10, 133–146.

25. Glaser, T., Brose, C., Franceschini, I., Hamann, K., Smorodchenko, A., Zipp, F., et al. (2007). Neural cell adhesion molecule polysialylation enhances the sensitivity of embryonic stem cell-derived neural precursors to migration guidance cues. Stem Cells 25, 3016–3025.

26. Kim, H.S., Choi, S.M., Yang, W., Kim, D.S., Lee, D.R., Cho, S.R., et al. (2014). PSA-NCAM(+) neural precursor cells from human embryonic stem cells promote neural tissue integrity and behavioral performance in a rat stroke model. Stem Cell Rev. 10, 761–771.

27. Gascon, E., Vutskits, L., Jenny, B., Durbec, P., and Kiss, J.Z. (2007). PSA-NCAM in postnatally generated immature neurons of the olfactory bulb: a crucial role in regulating p75 expression and cell survival. Development 134, 1181–1190.

28. Gammill, L.S., and Bronner-Fraser, M. (2003). Neural crest specification: migrating into genomics. Nat. Rev. Neurosci. 4, 795–805.

29. Sauka-Spengler, T., and Bronner-Fraser, M. (2008). A gene regulatory network orchestrates neural crest formation. Nat. Rev. Mol. Cell Biol. 9, 557–568.

30. Theveneau, E., and Mayor, R. (2012). Neural crest migration: interplay between chemorepellents, chemoattractants, contact inhibition, epithelial-mesenchymal transition, and collective cell migration. Wiley Interdiscip. Rev. Dev. Biol. 1, 435–445.

31. Cocchia, D., Polak, J.M., Terenghi, G., Battaglia, F., Stolfi, V., Gangitano, C., et al. (1983). Localization of S-100 protein in Muller cells of the retina--2. Electron microscopical immunocytochemistry. Invest. Ophthalmol. Vis. Sci. 24, 980–984.

32. Chambers, S.M., Fasano, C.A., Papapetrou, E.P., Tomishima, M., Sadelain, M., and Studer, L. (2009). Highly efficient neural conversion of human ES and iPS cells by dual inhibition of SMAD signaling. Nat. Biotechnol. 27, 275–280.

33. Basch, M.L., and Bronner-Fraser, M. (2006). Neural crest inducing signals. Adv. Exp. Med. Biol. 589, 24–31.

34. Hall, B.K., and Hall, B.K. (2009). The neural crest and neural crest cells in vertebrate development and evolution, 2nd edn (New York: Springer).

35. Tang, C., Lee, A.S., Volkmer, J.P., Sahoo, D., Nag, D., Mosley, A.R., et al. (2011). An antibody against SSEA-5 glycan on human pluripotent stem cells enables removal of teratoma-forming cells. Nat. Biotechnol. 29, 829–8

36. Ben-David, U., and Benvenisty, N. (2014). Chemical ablation of tumor-initiating human pluripotent stem cells. Nat. Protoc. 9, 729–740.

Abstract (in Korean)

전분화능 줄기세포 유래 신경능선세포의 분리, 특성 분석 및 이식

<지도교수 : 김 동 욱>

연세대학교 대학원 의과학과

이 동 진

인간 전분화능줄기세포(human pluripotent stem cells, hPSCs)의 발암 잠재력(tumorigenic potential)은 임상 적용에 있어서 중요한 문제이다. 현재까지는 종양 형성의 위험 요인을 최소화하고 제거하기 위해 인간 전분화능줄기세포를 특정한 세포로 선분화(pre-differentiation)하거나 표적 세포만 선별하여 분리시키는 전략이 이용되어 왔다. 그러나 인간 전분화능줄기세포 유래 신경전구세포를 중추 신경계(central nervous system, CNS) 질환 동물모델의 세포 치료에 이용하는 경우, 전분화능줄기세포가 검출되지 않음에도 반복적으로 종양이 형성되는 결과가 도출되었다. 이는 신경전구세포를 기반으로 한 이식치료의 위험인자를 확인하는 과정 중 중요한 신경 발달과정 중 하나인 다분화능 신경능선줄기세포(neural crest stem cells, NCSCs)의 발생을 간과했기 때문이었다. 본 연구는 신경전구세포 기반치료의 원천세포인 SOX1과 PAX6를 동시 발현하는 신경전구세포를 분석하여 polysialic acid-neural

cell adhesion molecule(PSA-NCAM) 음성세포가 초기 신경전구세포 배양 개체군을 오염시키며 이질성의 원인이 된다는 것을 밝히고, 그들이 종양 형성의 위험 요인이라는 것을 확인하였다. 또한 종합적인 분자 프로파일링, 글로벌 유전자 분석 및 유도분화를 통하여 PSA-NCAM 음성세포가 외/중배엽 계통으로 분화 가능한 다분화능 신경능선줄기세포임을 확인하였다. 본 연구에서 PSA를 PSA-NCAM 양성세포에서 제거하였을 때 신경능선줄기세포의 마커 발현이 증가하였고, PSA-NCAM 양성 그리고 음성세포를 단계적으로 혼합하여 쥐의 뇌에 이식하였을 때, 중배엽 유래 종양 및 PERIPHERIN 양성세포와 색소세포의 형성이 비례하여 증가하는 결과가 도출되었다. 따라서 본 연구를 통하여 신경능선줄기세포가 인간 전분화능줄기세포 유래 신경전구세포 기반치료에 있어 새로운 종양형성 인자임을 제안하며 중추 신경계에 이식치료 시 PSA-NCAM 음성세포를 제거하는 것이 발암 가능성을 억제한다고 판단한다.

핵심되는 말: 인간 전분화능줄기세포, 신경전구세포, 세포 치료, 종양 형성, 신경능선줄기세포, polysialic acid-neural cell adhesion molecule (PSA-NCAM)

PUBLICATION LIST

1. Park CY, Sung JJ, Choi SH, **Lee DR**, Park IH, Kim DW. Modeling and correction of structural variations in patient-derived iPSCs using CRISPR/Cas9. Nat Protoc. 2016 Oct; 11(11):2154-2169.

2. Park CY, **Lee DR**, Sung JJ, Kim DW. Genome-editing technologies for gene correction of hemophilia. Hum Genet. 2016 Sep;135(9):977-81.

3. Park CY, Halevy T, **Lee DR**, Sung JJ, Lee JS, Yanuka O, Benvenisty N, Kim DW. Reversion of FMR1 Methylation and Silencing by Editing the Triplet Repeats in Fragile X iPSC-Derived Neurons. Cell Rep. 2015 Oct 13;13(2):234-41.

4. **Lee DR**, Yoo JE, Lee JS, Park S, Lee J, Park CY, Ji E, Kim HS, Hwang DY, Kim DS, Kim DW. PSA-NCAM-negative neural crest cells emerging during neural induction of pluripotent stem cells cause mesodermal tumors and unwanted grafts. Stem Cell Reports. 2015 May 12;4(5):821-34.

5. Kim HS, Choi SM, Yang W, Kim DS, **Lee DR**, Cho SR, Kim DW. PSA-NCAM(+) neural precursor cells from human embryonic stem cells promote neural tissue integrity and behavioral performance in a rat stroke model. Stem Cell Rev. 2014 Dec;10(6):761-71.

6. Park CY, Kim HS, Jang J, Lee H, Lee JS, Yoo JE, **Lee DR**, Kim DW. ABCD2 is a direct target of β-catenin and TCF-4: implications for X-linked adrenoleukodystrophy therapy. PLoS One. 2013;8(2):e56242.

7. Kim DS, **Lee DR**, Kim HS, Yoo JE, Jung SJ, Lim BY, Jang J, Kang HC, You S, Hwang DY, Leem JW, Nam TS, Cho SR, Kim DW. Highly pure and expandable PSA-NCAM-positive neural precursors from human ESC and iPSC-derived neural rosettes. PLoS One. 2012;7(7):e39715.

8. Jang J, Yoo JE, Lee JA, **Lee DR**, Kim JY, Huh YJ, Kim DS, Park CY, Hwang DY, Kim HS, Kang HC, Kim DW. Disease-specific induced pluripotent stem cells: a platform for human disease modeling and drug discovery. Exp Mol Med. 2012 Mar 31;44(3):202-13.

9. Kim DS, Jung SJ, Nam TS, Jeon YH, **Lee DR**, Lee JS, Leem JW, Kim DW. Transplantation of GABAergic neurons from ESCs attenuates tactile hypersensitivity following spinal cord injury. Stem Cells. 2010 Nov;28(11):2099-108.